NASA TECHNICAL NOTE

NASA TN D-2599

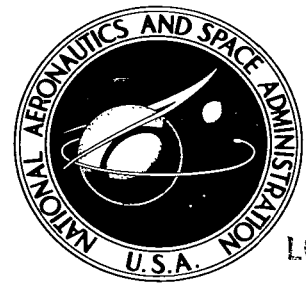

FRACTURE TOUGHNESS TESTING

by John E. Srawley and William F. Brown, Jr.

Lewis Research Center

Cleveland, Ohio

NATIONAL AERONAUTICS AND SPACE ADMINISTRATION • WASHINGTON, D. C. • JANUARY 1965

FRACTURE TOUGHNESS TESTING

By John E. Srawley and William F. Brown, Jr.

Lewis Research Center
Cleveland, Ohio

NATIONAL AERONAUTICS AND SPACE ADMINISTRATION

For sale by the Office of Technical Services, Department of Commerce,
Washington, D.C. 20230 -- Price $3.00

CONTENTS

FRACTURE TOUGHNESS TESTING

by John E. Srawley and William F. Brown, Jr.

Lewis Research Center

SUMMARY

A comprehensive survey is presented of current methods of fracture toughness testing that are based on linear elastic fracture mechanics. General principles are discussed in relation to the basic two-dimensional crack stress field model and in relation to real three-dimensional specimens. The designs and necessary dimensions of specimens for mixed mode and opening mode (plane strain) crack toughness measurement are considered in detail. Methods of test instrumentation and procedure are described. Expressions for the calculation of crack toughness values are given for the common types of specimens.

INTRODUCTION

The survey of fracture toughness test methods herein will be restricted to those methods that have their basis in linear elastic fracture mechanics, or that can be treated satisfactorily by the methods of linear elastic fracture mechanics at the present time. This restriction of scope carries with it no implication that there are not other methods worthy of consideration. In the opinion of the authors, some of the arbitrary empirical procedures for evaluating fracture toughness are, and will continue to be, of great value, having been proved by correlation with service failure studies (refs. 1 and 2). In particular note the work of Pellini and his colleagues at the U.S. Naval Research Laboratory (refs. 3 and 4). The prime purpose herein, however, is to clarify the test methods of linear elastic fracture mechanics. From a practical point of view, the arbitrary empirical procedures (the most familiar being notched-bar transition-temperature testing) are most useful for evaluating structural steels in the lower range of yield strengths. The application of steels in the higher range of yield strengths and of titanium and aluminum alloys calls for much more discriminating evaluation to the point of being able to estimate the strength of structural elements containing cracks. Thus, it is desirable that fracture toughness testing of such materials shall be based on the principles of mechanics as applied to cracked bodies.

Because of its rapid development over the last decade or so, fracture mechanics has seemed confusing to many interested parties. It is therefore useful to keep in mind the basic essentials of the discipline. In the simplest terms, the fracture toughness of a material determines how large a crack the material is able to tolerate without fracture when loaded to a level approach-

ing that at which it would fail by excessive plastic deformation. For example, how large a crack can be tolerated in the wall of a pressure vessel manufactured from Brand X steel when the nominal hoop stress is raised to 90 percent of the yield strength?

Naturally, every reasonable effort would be made to avoid having any cracks or like defects in the structure. But grievous experience indicates unmistakably that it would be quite unrealistic to depend upon the total absence of cracklike defects. If something fairly quantitative about the crack tolerance of materials were known, more realistic and more effective measures could be taken with regard to inspection, quality control, proof testing, and avoidance of development of cracks in service. For instance, the material having the greatest crack tolerance at the stress level contemplated could be selected out of those that have adequate yield strength and are satisfactory in other respects. Or it could be decided, according to the application in mind, how far weight and bulk could be reduced by employing materials of greater yield strength at the expense of reduced crack tolerance. In this connection, the dimensions of cracks that have been discovered to be the origins of fracture failures of critical structures range from a few thousandths of an inch, in the case of some steels with yield strengths approaching 250,000 psi, up to more than a foot in diameter, in the case of at least one low strength steel casting.

The most direct way of evaluating the crack tolerance of a material apparently would be to test a series of specimens provided with cracks of graded sizes to determine an empirical relation between strength and crack size. But the problem is not simply a matter of crack size. In addition, crack shape, bulk of the member (i.e., thickness of a plate) orientation of the crack in relation to the fibering of the material, temperature, and rate of loading all may affect the fracture strength of a structural member of a given material. To take into account all these factors in a purely empirical test program would require very large numbers of specimens for each material evaluated. The burden of testing can be considerably reduced, however, by applying knowledge of the mechanics of fracturing, best represented at the present time by linear elastic fracture mechanics.

For the following discussion some familiarity is assumed with the concepts, assumptions, and stress analysis aspects of current linear elastic fracture mechanics. For additional information, reference can be made to the reports of the ASTM Special Committee on Fracture Testing of High Strength Metallic Materials (refs. 5 to 9), hereinafter referred to as the ASTM Special Committee on Fracture Testing. In these references, the discussion is often in terms of K, the stress intensity factor of the elastic stress field local to the crack, rather than in terms of $\mathcal{G}$, the crack extension force, or strain energy release rate with respect to crack extension. For reasons that will become apparent it is more convenient in this dissertation to develop our subject primarily in terms of $\mathcal{G}$ rather than K. This should cause no difficulty if the simple relations between these two quantities are kept in mind: $K^2 = E\mathcal{G}$ for plane stress, and $K^2 = E\mathcal{G}/(1 - \nu^2)$ for plane strain, where E is Young's modulus and ν is Poisson's ratio. (All symbols are defined in appendix B.)

A satisfactory fracture toughness test, in the present context, is simply

a model fracture experiment designed to satisfy two essential requirements, namely, (1) the specimen dimensions and loading arrangement must be such that the value of the crack extension force $\mathcal{G}$ can be calculated with sufficient accuracy at any stage of the test at which the values of the load and the crack dimensions are known and (2) the values of the load and the crack dimensions at the point of instability of crack extension can be measured with sufficient accuracy. As will be shown later, it follows from the first of these requirements that the crack dimensions, and therefore the dimensions of the specimen in which it is contained, must exceed certain minimum values that increase as the ratio of $E\mathcal{G}_c$ to the square of the yield strength of the material. Since there is a general tendency for $\mathcal{G}_c$ to increase as the level of yield strength of structural materials is decreased, it follows further that the minimum necessary dimensions of a specimen of a given type increase very rapidly as the yield strength level of the materials to be tested decreases. To illustrate this point, whereas the overall diameter of the smallest circumferentially crack-notched round bar necessary to measure the plane strain crack toughness $\mathcal{G}_{Ic}$ of a steel having a yield strength of 300,000 psi would probably be less than 0.2 inch, the smallest diameter necessary for a steel having a yield strength of 150,000 psi might exceed 5 inches.

In order to minimize specimen dimensions as much as possible, thereby making most effective use of available test material and testing machine loading capacity, types of specimens have been developed in which the dimensions of the simulated crack are appreciable fractions of the overall specimen dimensions. The expressions for $\mathcal{G}$ for such specimens are necessarily more complicated than the simple expression $E\mathcal{G} = \pi\sigma^2 a$, which applies to a straight, through-thickness crack of length $2a$ in a flat plate of width W greater than $20a$, under uniform tensile stress σ. Sufficiently accurate approximate expressions have been obtained by mathematical or experimental methods for a number of useful types of specimens discussed later. These include specimens that are loaded in bending as well as in tension.

While linear elastic fracture mechanics is probably about the simplest form of strength-of-materials approach that could be taken in the study of fracturing phenomena, it is nevertheless quite a complex subject. This results from the inherent complexity of the fracture behavior of actual materials. Consequently, the subject of fracture toughness testing will be developed in stages, starting with a simple, idealized model of a fracture toughness test specimen that is referred to as the quasi-two-dimensional prototype specimen. This is an abstraction of the wide plate specimen referred to in the preceding paragraph in which the thickness of the plate is ignored. This will allow development of the important concepts of crack-extension resistance and fracture instability in essentially two-dimensional terms. Next are considered the complications associated with finite thickness and the change in fracturing behavior and apparent toughness as the thickness is varied through the transition from slant, or plane stress, fracture mode to square, or plane strain fracture mode. This leads to consideration of the measurement of plane strain crack toughness $\mathcal{G}_{Ic}$, which is of particular importance in that it represents a practical lower limit to the fracture toughness of a material under given conditions. It is then appropriate to consider practical specimen types that require reasonable amounts of material and loading capacity. The narrow symmet-

rical plate types of specimen for general $\mathcal{G}_c$ testing are discussed first, and then several types of specimens suitable for $\mathcal{G}_{Ic}$ testing only are discussed in sequence. In these sections, the question of $\mathcal{G}_c$ measurement capacity in relation to specimen size is discussed for each type of specimen. Table I (p. 36) is provided for comparison of the various types of $\mathcal{G}_{Ic}$ measurement specimens. In the remaining sections the topics of test instrumentation and procedure and certain aspects of specimen design and preparation are discussed. Appendix A provides ready reference information on the various types of specimens, giving proportioned sketches and appropriate expressions for $\mathcal{G}$ in compact form in each case.

GENERAL CONSIDERATIONS

QUASI-TWO-DIMENSIONAL PROTOTYPE SPECIMEN

It is desirable to discuss the general concepts that apply to all fracture mechanics type toughness tests before considering in detail the various types of fracture toughness test specimens that are in common use. First, consideration is given to a simple, idealized model and then the various complications encountered with real specimens are introduced systematically. This model is called a quasi-two-dimensional prototype specimen, and it may be visualized as a flat sheet of width W under uniform uniaxial tension σ, and containing a straight, ideal crack of length $2a$ less than $W/10$ in the center and normal to the direction of the applied stress. The thickness is regarded as vanishingly small and the length sufficient so that the stress field disturbance due to the crack is insignificant at the ends.

This model is an idealization of an otherwise similar plate specimen of finite thickness B. For such a real specimen, discussed later, the crack front configuration may be quite complex, and $\mathcal{G}$ (the crack extension force per unit length of crack border, or strain energy release rate with crack extension per unit length of crack border) has, in general, a different value at each position along the crack border. With the quasi-two-dimensional model only a single value of $\mathcal{G}$ needs to be considered, which may be regarded as a sort of average value for the real crack in the plate of finite thickness. The state of the stress field is assumed to be one of generalized plane stress, and the appropriate expression for $\mathcal{G}$ is $E\mathcal{G} = \pi\sigma^2 a$ (ref. 10).

Criterion of Fracture Instability

In a typical fracture toughness test, the load on the specimen is raised continuously until a point is reached at which unstable crack extension occurs. In order to define this more precisely, it has to be appreciated that the load is not the independent variable in the test. The variable that is actually most nearly under the control of the operator is the separation of the heads of the testing machine. For the present purpose, this separation can be regarded as equivalent to the overall extension of the specimen e, which will be taken as the independent test variable. (In the case of a bend specimen, e would be the specimen deflection.) The criterion for the point of instability of crack extension in the test is then that the load P, as a function of e, reaches a

stationary value, that is, either a maximum or a point of inflection of zero slope. In mathematical terms, $dP/de = 0$. At this point the ability to control the load is lost, at least temporarily, and that is why the load cannot be regarded as the independent variable.

The value of $\mathcal{G}$ at the point of instability can be calculated from measurements of the load and the instantaneous crack length at that point and is designated $\mathcal{G}_c$. Either $\mathcal{G}_c$ or K_c (equal to the square root of $E\mathcal{G}_c$ for plane stress conditions) is taken as a measure of fracture toughness of the material.

This operational definition of the point of instability of crack extension, and the corresponding definitions of $\mathcal{G}_c$ and K_c, correspond to those adopted by the ASTM Special Committee on Fracture Testing (ref. 5). To correct a common misapprehension, $\mathcal{G}_c$ and K_c are not necessarily independent of specimen dimensions other than thickness, as will be shown in the next section. Nevertheless, they do have useful quantitative significance as measures of fracture toughness.

In some of the literature on fracture mechanics $\mathcal{G}_c$ is defined in different terms, for instance, as the value of the crack extension force at the onset of rapid crack propagation. Such a definition is too vague as an operational definition for testing purposes and may be even somewhat misleading in seeming to imply that continuing slow crack extension is to be expected at constant levels of $\mathcal{G}$ less than $\mathcal{G}_c$. Such behavior, fortunately, is unusual and when observed indicates a need for careful investigation of the material and the environment in which the test is conducted. To avoid ambiguity in conducting and interpreting fracture toughness tests, the precise operational definition of $\mathcal{G}_c$ is to be preferred.

Crack Extension Resistance and Occurrence of Instability

To appreciate the conditions that must be satisfied in valid fracture toughness tests, and to understand properly the results that are obtained, it is necessary to be familiar with the current concept of the growth of resistance to crack extension during a test. This concept was originated by G. R. Irwin (ref. 11), and is mentioned in the first report of the ASTM Special Committee on Fracture Testing but has not been given much emphasis heretofore. The most extensive previous discussion is probably that given by Krafft, Sullivan, and Boyle (ref. 12).

The essence of this concept is that, as the crack extension force $\mathcal{G}$ is increased during a test, it is opposed by an increasing resistance to crack extension R of the material at the crack tip, so that equilibrium between $\mathcal{G}$ and R is maintained up to the point of instability. The crack extension resistance R may be thought of as analogous to the increasing resistance to plastic deformation due to work hardening, which opposes the applied stress in an ordinary tension test. In this case also there is a point of instability at which $dP/de = 0$.

By definition, $\mathcal{G}_c$ is equal to the value of R at instability and beyond this point $\mathcal{G}$ increases more rapidly with e than does R. Now, although the values of $\mathcal{G}$ and R are equal up to the point of instability, these quantities represent distinctly different physical entities and have different functional relations to the subsidiary test variables σ and a. For the prototype specimen, as noted earlier, $\mathcal{G} = \pi\sigma^2 a/E$, but the dependence of R on these variables has yet to be discussed. First, it should be noted that there is a condition which must be satisfied at the point of instability that may be derived as follows: Since $\mathcal{G}$ - R is equal to zero up to the point of instability, $d(\mathcal{G} - R)$ is also equal to zero up to this point. Expressing this in terms of the subsidiary variables σ and a yields

$$\frac{d(\mathcal{G} - R)}{de} = 0 = \frac{\partial \mathcal{G}}{\partial \sigma}\frac{d\sigma}{de} + \frac{\partial \mathcal{G}}{\partial a}\frac{da}{de} - \frac{\partial R}{\partial \sigma}\frac{d\sigma}{de} - \frac{\partial R}{\partial a}\frac{da}{de} \tag{1}$$

At instability, $d\sigma/de = 0$ by definition, and equation (1) reduces to

$$\left(\frac{\partial \mathcal{G}}{\partial a}\right)_{\sigma=\sigma_c} = \left(\frac{\partial R}{\partial a}\right)_{\sigma=\sigma_c} \tag{2}$$

where σ_c is the stationary value of σ at instability.

The significance of this is illustrated in figure 1, which shows a plane section through the surface representing $\mathcal{G}$ as a function of σ and a for the constant value of σ equal to σ_c. In the simple case of the prototype specimen, the trace of the $\mathcal{G}$ surface is the straight line $\mathcal{G} = \pi\sigma_c^2 a/E$ as shown. In general, it would be an upward sweeping curve. The curve representing R in the figure is a projection onto the plane section of a three-dimensional curve representing a relation, as yet unspecified, between R, σ, and a. This three-dimensional curve must lie in the $\mathcal{G}$ surface up to the point of instability if R is equal to $\mathcal{G}$ up to this point. Equation (2) expresses the condition that the trace of the $\mathcal{G}$ surface in figure 1 must be tangent to the projection of the R curve at the point of instability. A similar figure for a constant value of σ less than σ_c would show the $\mathcal{G}$ surface trace intersecting the projection of the R curve.

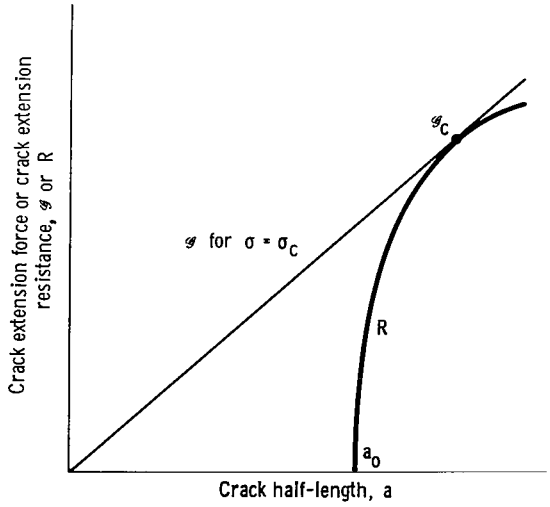

Figure 1. - Section at constant $\sigma = \sigma_c$ through surface representing $\mathcal{G}$ as function of σ and a for prototype specimen, showing projection of curve representing crack extension resistance R tangent to line representing $\mathcal{G}$ at point $\mathcal{G}_c$. Form of R curve was arbitrarily assumed.

In a fracture toughness test, as normally conducted, the value of only one point on the crack extension resistance curve is determined, namely, the instability point for the particular specimen used, which is called $\mathcal{G}_c$. This is something like determining only the ultimate tensile strength in an ordinary tension test. How nearly independent of

crack length $\mathcal{G}_c$ will be for a group of tests on the same material, but for specimens with different initial crack lengths, will depend upon the form of the R curve for the material. To characterize the fracture toughness of a material thoroughly, it would be necessary to determine the entire R curve. Fortunately, experience suggests that $\mathcal{G}_c$ is sufficiently independent of crack length to provide a single-valued representation of the fracture toughness of most materials for most practical purposes. Where this is not the case, the R curve can be determined by using a sufficiently large specimen and can be used for a more detailed study of a potential fracturing situation than would be possible from a knowledge only of a single $\mathcal{G}_c$ value.

The only published data on R curves seem to be those given in reference 12 for aluminum 7075.T6. Consequently, very little is known, in general, about the forms of R curves and the factors upon which they depend. Krafft, et al., however, have proposed a very plausible working hypothesis that is consistent with the observations of reference 12 and which will be utilized herein. The hypothesis can be stated as follows: For a given material in an inert environment under given conditions of testing speed and temperature, the resistance to crack extension R is primarily a function of the magnitude of crack extension $a - a_o$ and is independent of the initial crack length $2a_o$. This implies also that R is not directly a function of σ, only indirectly in that both R and σ are related to $a - a_o$. This hypothesis refers to an ideally sharp starting crack and, in effect, assumes that an invariant sequence of development of crack front configuration and associated plastic zone occurs as $a - a_o$ increases, whatever the value of $2a_o$. Study of the fracture surfaces of specimens having different initial crack lengths lends considerable support to this concept of an invariant pattern of development for specimens of the same thickness. At this point the question of thickness is still neglected, but will be dealt with in a later section.

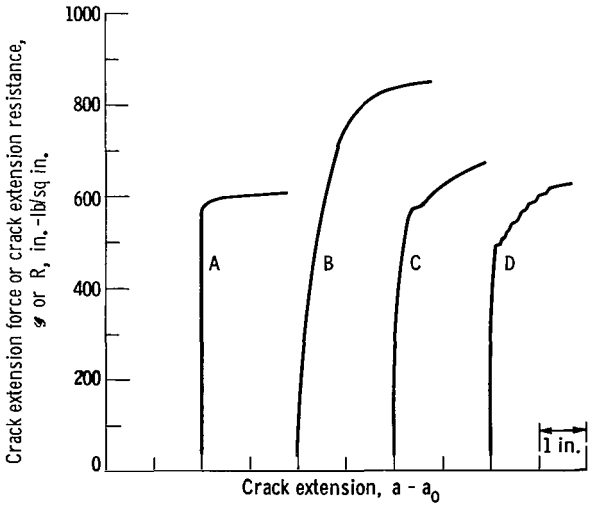

Figure 2. - Some conceivable types of crack extension resistance curves. A - Sharply defined instability. B - Representative of actual behavior of Al 7075.T6 according to reference 12. C - Transient instability due to sudden extension in opening mode ("pop-in") followed by further, mixed-mode, stable crack extension. D - Discontinuous growth of crack extension resistance, characteristic of real materials to some degree. Other examples are actually smoothed versions of this sort of behavior.

If the working hypothesis described in the previous paragraph is accepted, the approximate form of the R curves for a variety of materials can be inferred from unpublished data obtained by the present authors. Figure 2 shows some examples, curves A, B, and C, representing smoothed versions of actual behavior. The curves for real materials are always more or less erratic on a fine scale, as indicated by curve D. Curve A represents a case approaching ideal brittle behavior, in which case $\mathcal{G}_c$ would be virtually invariant. This point is illustrated in figure 3, which shows the points of tangency of $\mathcal{G}$ traces to R curves of type A for several different initial crack lengths. This figure, and others

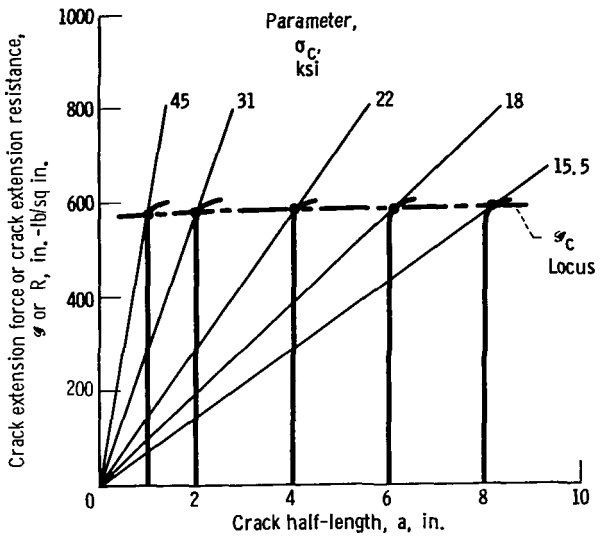

Figure 3. - Showing near-invariancy of $\mathcal{G}_c$ as function of initial crack length for material having crack extension resistance curve of near-ideal-brittle type.

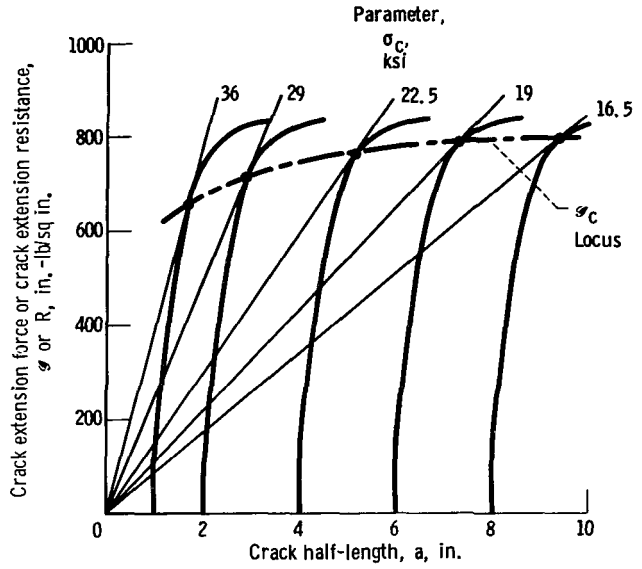

Figure 4. - Showing dependence of $\mathcal{G}_c$ on initial crack length for material having crack extension resistance curve of type B, figure 2 (representative of Al 7075.T6).

that follow are representations of the same kind as figure 1. In figure 3, the R curves are identical except for lateral displacements of the origins to different values of the initial crack half-length. For this type of R curve, $\mathcal{G}_c$ is almost constant, the locus tending to slightly lower values for shorter initial crack lengths. In practice, behavior of this sort is to be expected when the specimen breaks with a square, brittle-appearing fracture.

Figure 4 is a plot similar to figure 3 except that the R curve is that shown as type B in figure 2. This curve is a good fit to the data for aluminum 7075.T6 reported in reference 12. The dependence of $\mathcal{G}_c$ on initial crack length is quite considerable in this case compared with that shown in figure 3. When specimens are used for which $2a_o$ is about 0.3 W or greater, the situation is further complicated and $\mathcal{G}_c$ may have a maximum value at some value of $2a_o$, as will be shown later.

To summarize thus far, some of the general aspects of fracture mechanics toughness testing have been considered by referring to a quasi-two-dimensional prototype model specimen that has deferred consideration of some of the complexities involved when real specimens are considered. An operational definition has been given for the point of instability of crack extension in a test, and $\mathcal{G}_c$ has been defined as the value of the crack extension force at that point: K_c is defined similarly. The concept of crack extension resistance R has been discussed, and the working hypothesis that R is primarily a function of the magnitude of crack extension $a - a_o$, independent of initial crack length, has been assumed. On this basis it has been shown that $\mathcal{G}_c$ may depend to some extent on the initial crack length, the extent of the dependence varying according to the form of the R curve for the material. Thus, $\mathcal{G}_c$ is not to be regarded as an invariant property of the material, but rather as a somewhat arbitrary underestimate of the limiting value of R for a long crack

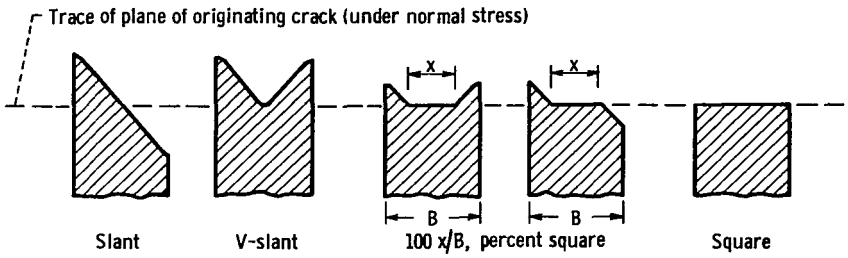

Figure 5. - Recommended descriptive terms for types of fracture surfaces observed in plate specimens illustrated by section views taken normal to direction of propagation.

in a wide plate of the material.

ACTUAL CRACKS IN SPECIMENS OF FINITE THICKNESS

Real, wide-plate specimens of finite thickness B, in other respects similar to the quasi-two-dimensional prototype, will be considered here. Anyone familiar with fractures of plate specimens knows the common forms that they might take, as illustrated by schematic section views in figure 5. The two extreme types of fracture are referred to here by the terms slant and square in preference to the more usual terms shear and flat. The term shear is misleading because this type of fracture does not necessarily occur by relative displacement of the two surfaces in their common plane, and the term flat is ambiguous because a slant fracture can be as flat as a square fracture.

Since only the extreme slant and square types of fracture surface are roughly flat, it is clear that the front of an extending crack in a real plate is not even roughly represented by a straight line, except possibly in the extreme cases. Actually, as is well known, the front of a square fracture is roughly parabolic with the most advanced point at midthickness. For a fully developed slant fracture, the front is almost straight, as shown in figure 6(a). This has been established by terminating tests of steel specimens at a point short of instability. In each case, the specimen was removed from the testing machine, heat tinted to mark the crack boundary (the use of a liquid staining medium for this purpose is not reliable), then loaded again to complete the fracture. In the general case of a mixed fracture consisting of a central square strip with slant borders, the crack front must be a nonplanar curve. A good example of this case, obtained by the heat-

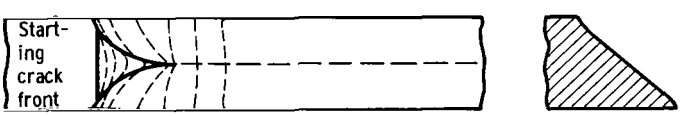

(a) Fully developed slant fracture.

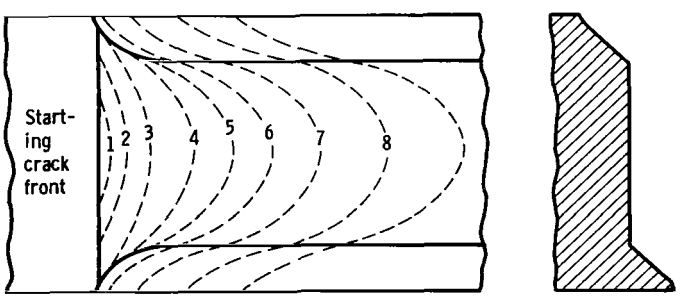

(b) Predominantly square fracture.

Figure 6. - Schematic drawing of various successive positions of crack fronts, shown as dashed lines, in specimens having fully developed slant fracture and predominantly square fracture (about 70 percent square).

tinting procedure, is illustrated in reference 13.

The value of $\mathcal{G}$ for a given load varies with position along the crack front according to the curvature at that position. Unfortunately, no detailed analysis has been made for a curved front of a through-thickness crack in a plate, though some insight can be gained by reference to Irwin's discussion of the case of a semielliptical part-through crack (ref. 14). Consequently, it has to be assumed that a single average value of $\mathcal{G}$ can be taken to apply to the whole crack front with sufficient accuracy for practical purposes. Essentially, the finite thickness plate is treated in the same way as the quasi-two-dimensional prototype specimen, and it is important to realize this because the generalized plane stress model is only an approximation to the real specimen, even in the case of a thin sheet specimen fracturing with a fully developed slant fracture. Where apparent inconsistencies in test results occur, the adequacy of this model to represent the actual test specimen should be carefully reconsidered.

The assumption of an average value of $\mathcal{G}$ involves some assumption about the value of the effective crack length $2a$ to be used in calculating $\mathcal{G}$. This will depend on the method of measurement and will be discussed in a later section. It also involves the use of a plastic zone correction term, also discussed later. At this point it is sufficient to note that uncertainty about the value of $2a$ at instability is the largest source of error in $\mathcal{G}_c$ measurements.

Dependence of $\mathcal{G}_c$ and Fracture Appearance on Thickness

For a given material at a given temperature and testing speed, both the appearance of the fracture of a plate specimen and the $\mathcal{G}_c$ value will depend on the thickness. This dependence is not the result of the metallurgical processing involved in reducing the plate to various thicknesses because the effect can be demonstrated by testing specimens of different thicknesses obtained by machining from plate stock of the same initial thickness. Metallurgical processing effects may also occur, but these should not be confused with the intrinsic effect of thickness.

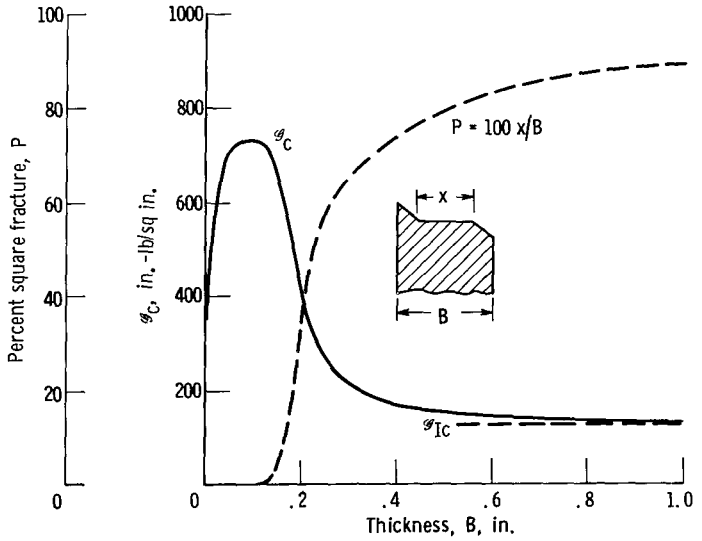

Figure 7. - Dependence of $\mathcal{G}_c$ and fracture appearance (in terms of percent square fracture) on thickness of plate specimens. Schematic, but based on data for aluminum 7075.T6.

The intrinsic effect of thickness is illustrated in figure 7, which is based on data for aluminum 7075.T6 from reference 15. The curve is qualitatively typical of many high-strength metallic materials.

The quantitative aspects, such as the peak value of $\mathcal{G}_c$, the lower limiting value for large thickness $\mathcal{G}_{Ic}$, the thickness at which $\mathcal{G}_c$ is greatest, and the range of thickness over which the major part of the fracture mode transition occurs are all dependent upon the material and the testing temperature (and, in some cases, on the speed of testing). For a particular material at a particular temperature, these aspects depend upon the yield strength level when this is varied by thermal or mechanical treatment.

The initial, ascending portion of the curve of $\mathcal{G}_c$ as a function of thickness is associated with fractures that are fully slant or V-slant, and is commonly explained by assuming that the volume of associated plastically deformed material per unit length of fracture is proportional to the square of the thickness. This follows from the assumption that the patterns of plastic deformation for different thicknesses in this range are geometrically similar, which agrees with observation. If it is further assumed that the density of plastic deformation energy is constant throughout the plastically deformed volume, the plastic work per unit thickness per unit crack extension, which is equated with $\mathcal{G}_c$, is directly proportional to the thickness. Actually, the available data are only sufficient to confirm that $\mathcal{G}_c$ does increase with thickness in this range, not to confirm any particular form of the relation. It seems unlikely that there should be a simple linear dependence.

The descending portion of the curve of $\mathcal{G}_c$ as a function of thickness is associated with the occurrence and progressive dominance of square fracture surface in the center of the plate thickness. At sufficiently large thicknesses, the slant-fracture borders occupy a negligible proportion of the total fracture surface, and $\mathcal{G}_c$ approaches a lower limiting value $\mathcal{G}_{Ic}$, referred to as the plane strain fracture toughness or the opening mode fracture toughness. In the case of square fracture, it is usually assumed that the layer of associated plastically deformed material extends for a constant distance from the fracture surface, independent of the plate thickness. Also, with the assumption that the density of plastic deformation energy depends only upon the distance from the fracture surface, the plastic work per unit thickness per unit crack extension $\mathcal{G}_{Ic}$ will be independent of thickness for a completely square fracture (refs. 12 and 16).

The roman numeral subscript I refers to the first of three component modes of crack extension distinguished by G. R. Irwin (refs. 17 to 19). In this mode the mating crack surfaces separate as the crack extends so that their relative displacement is normal to the fracture plane; hence, it is called the opening mode. It corresponds to the intuitive concept of cleavage separation (but should not be confused with cleavage in a microcrystalline sense). Modes II and III are referred to as the edge sliding mode and the screw sliding mode, respectively (analogous to the concepts of edge and screw dislocations in crystals). In the two sliding component modes, there is no relative displacement of the mating crack surfaces in the direction of their normal; the surfaces are supposed to slide over one another either in the direction of crack extension or normal to it. Any arbitrary mode of crack extension can be represented as a linear combination of these three component modes, and the three quantities $\mathcal{G}_I$, $\mathcal{G}_{II}$, and $\mathcal{G}_{III}$ are the corresponding rates of transfer with crack extension of energy from the surrounding elastic strain field to other forms (ref. 17).

From a macroscopic point of view, square fractures are usually considered to result from simple mode I crack extension in a gross sense. In microscopic detail, they are quite complex and may involve a variety of fracture modes. In practice, $\mathcal{G}_{Ic}$ refers to the gross average toughness value for macroscopic opening mode crack extension. Slant fractures that occur when specimens are loaded in tension (in contrast to torsion) are not the result of pure sliding mode crack extension in a gross sense. As can be deduced by observing such specimens during tests, the component of relative displacement normal to the crack surfaces is considerable. Fractographic examination confirms that this must be so because the ductile dimples observed on slant-fracture surfaces of specimens broken in tension are not generally pronouncedly elongated in one particular direction (ref. 20).

The plane strain, or opening mode, crack toughness $\mathcal{G}_{Ic}$ is of special importance in that it represents a practical lower limit to the fracture toughness of a material in a given condition and at a given temperature and rate of testing. The possibly lower values of $\mathcal{G}_c$ for very small thicknesses are only rarely of practical importance, and apparently no such values have yet been measured for any material. There are many practical applications where the fracture, if it occurred, would be virtually completely square, and the relation of load-bearing capability to crack dimensions would be governed by $\mathcal{G}_{Ic}$. Even when the section of the load-bearing member is thin enough so that the fracture would be partly or entirely slant, the load-bearing capability might be governed by $\mathcal{G}_{Ic}$ rather than by the value of $\mathcal{G}_c$ measured for the actual thickness, unless the ratio $\mathcal{G}_c/\mathcal{G}_{Ic}$ exceeded some value that would depend on the shape and size of the initial crack. More detailed discussion of this point is given in references 6 and 19.

From the point of view of having a single value representing the fracture toughness of a material, $\mathcal{G}_{Ic}$ is independent of the dimensions of the specimen (provided that these are sufficiently large for a proper $\mathcal{G}_{Ic}$ measurement) in contrast to $\mathcal{G}_c$, which depends strongly on thickness and to some extent on crack length, as has been shown. Of course, materials exhibit nonuniformity and anisotropy with respect to $\mathcal{G}_{Ic}$, just as they do for other properties, and this has to be taken into consideration in evaluating a material. In general, in the absence of more specific information, it will always be a safe practice to use a properly determined value of $\mathcal{G}_{Ic}$ as the measure of the toughness of a material, except possibly in some cases of very thin sheet or foil.

$\mathcal{G}_{Ic}$ Measurement at Metainstability or "Pop-in"

The most obvious way to measure $\mathcal{G}_{Ic}$ would be to test a sufficiently thick plate specimen of the material. This might not always be convenient, or even possible, and certainly would not be very economical of material. Because of the importance of $\mathcal{G}_{Ic}$, a number of different types of specimens have been developed for measuring it. At this point it is convenient to discuss the concept of metainstability and the so-called pop-in method of measuring $\mathcal{G}_{Ic}$, which applies to several of these types of specimens and which makes it possible to use thinner specimens than would be required to obtain an almost entirely square fracture.

The pop-in method of $\mathcal{G}_{Ic}$ determination was first proposed by Boyle, Sullivan, and Krafft (ref. 21), who observed in tests of sheet specimens of aluminum 7075.T6 that the first appreciable extension of the crack occurred as a distinct burst or pop-in that was then followed by a stage of gradual crack extension as the load was further increased. The same phenomenon had been observed by numerous other investigators in the form of an audible ping or click at the pop-in load, but its significance had apparently not been appreciated. Boyle, et al. (ref. 21) were able to show that the value of $\mathcal{G}$ at pop-in was essentially the same as the value of $\mathcal{G}_{Ic}$, which would be determined with a sufficiently thick plate specimen.

The term pop-in is descriptive of what actually occurs, namely, an abrupt extension of the crack front from its initial position to some position such as that labeled 5 in figure 6(b) (p. 9), while the load remains constant or even drops slightly. The crack movement can be followed during a test by using the output from either an electrical potential measuring device or a displacement gage to drive an X-Y recorder, as discussed in the sections ELECTRICAL POTENTIAL MEASUREMENT and DISPLACEMENT GAGES. Figure 8 shows three contrasting examples of electric potential change at constant current as a function of load for specimens of maraging steel 0.2 inch thick. Example A represents material aged 3 hours at 600° F, B aged at 1000° F, and C aged at 800° F. The arrows indicate interruption of the tests for heat tinting to mark the crack front positions. Whereas example C exhibits very distinct pop-in behavior, example B is somewhat ambiguous, and example A is apparently not interpretable in terms of pop-in at all. In the case of example C, the heat-tinting procedure showed that the shape of the crack front after pop-in was approximately that shown as position 5 in figure 6(b), although the fracture in this case was less than 50 percent square. These three examples serve to make the further point, discussed later, that distinct pop-in behavior is not always observed and therefore cannot be depended on for $\mathcal{G}_{Ic}$ measurement in all cases.

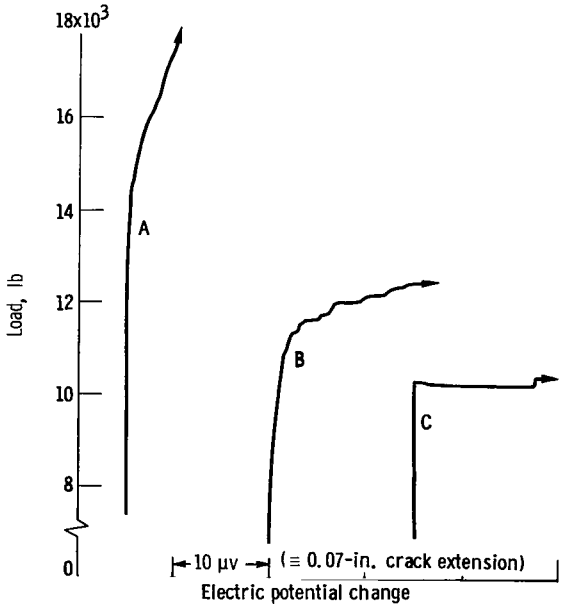

Figure 8. - Three typical examples of change in electric potential as function of load during test of single-edge-notch tension specimens. There is good correlation between electric potential change and crack extension. Specimens were maraging steel aged 3 hours at 600° F, A; 1000° F, B; and 800° F, C.

When pop-in does occur it satisfies the instability condition $d\sigma/de = 0$, but the instability is only temporary, so that it is referred to as metainstability. It will now be considered in terms of the crack extension resistance curves discussed earlier. Figure 9 shows a projected curve of R against a, which is derived from the records of tests of the maraging steel aged 3 hours at 800° F, the records being similar to example C of figure 8, but carried to more advanced stages. As the specimen is extended, the slope of the $\mathcal{G}$ against a trace increases in proportion to σ^2. The $\mathcal{G}$ trace intercepts the

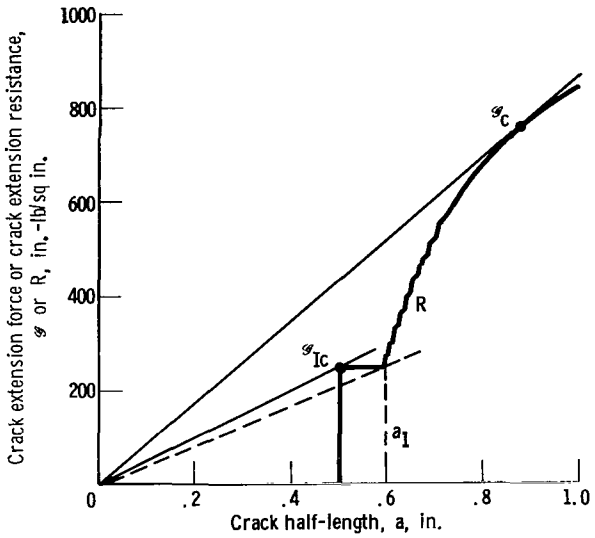

Figure 9. - Metainstability at $\mathcal{G}_{Ic}$ and ultimate instability at $\mathcal{G}_c$ for wide plate specimen of material exhibiting pronounced pop-in behavior, as indicated by marked step in curve of R against a. Schematic; but pop-in behavior based on actual tests of maraging steel aged 3 hours at 800° F.

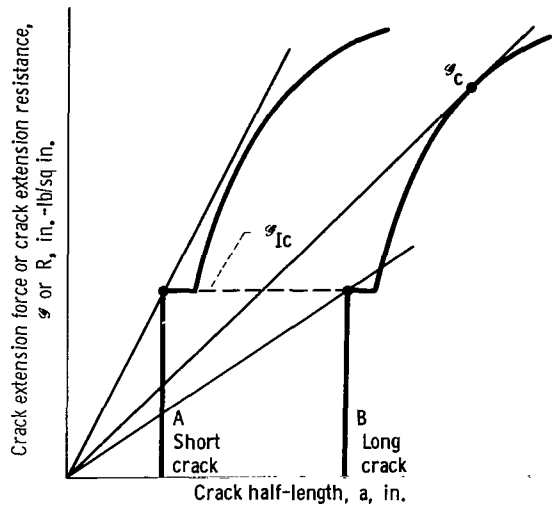

Figure 10. - Behavior of two wide plate specimens of same material and thickness having considerably different initial crack lengths: A, short crack, specimen breaks at load corresponding to $\mathcal{G}_{Ic}$; B, long crack, ultimate load is considerably higher than that corresponding to $\mathcal{G}_{Ic}$.

R curve so that equilibrium is maintained until the step in the R curve is reached. At this point the value of R over a certain interval of $a - a_o$ is less than the value of $\mathcal{G}$ corresponding to the stress at the point $\mathcal{G}_{Ic}$. Thus, the balance between $\mathcal{G}$ and R is temporarily upset until the crack has extended to the point a_1 or somewhat beyond. The extent to which the load drops in this interval is a function of several variables. However, $\mathcal{G}$ and R will again become balanced at some value of a slightly greater than a_1 and will remain so, on the average, until the point $\mathcal{G}_c$ is reached. Beyond this point, the load cannot increase further, and, even though extension of the specimen is halted at this point, the excess of $\mathcal{G}$ over R will continue to increase with increasing a, so that crack extension accelerates under the driving force of the excess elastic strain energy of the system. This may be referred to as the ultimate instability point of the test as distinguished from the metainstability that occurs at $\mathcal{G}_{Ic}$.

One of the consequences of the hypothesis that the value of R is a function of $a - a_o$ only is illustrated in figure 10. This represents two wide plate specimens, supposedly identical except that the initial crack lengths are different. The R curves are therefore identical but originate at different values of a_o. The behavior of the specimen with the longer crack, curve B, is the same as that described in connection with figure 9. The behavior of the specimen with the shorter crack, curve A, will be different in that ultimate instability will be reached at $\mathcal{G}_{Ic}$; that is, the load cannot increase beyond the value reached at pop-in. If extension of the specimen is maintained at a steady rate, the load will drop at pop-in, then may increase again slightly, but the load at which $\mathcal{G}$ and R are equal at any subsequent stage of crack extension will always be less than the pop-in load. Thus, the load-bearing capability of the specimen is controlled by $\mathcal{G}_{Ic}$ and not by some higher value

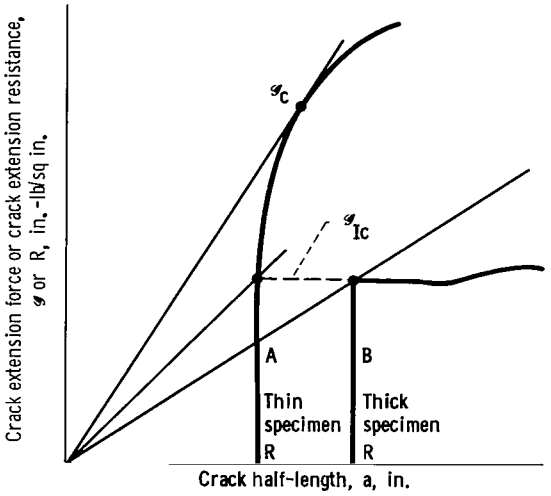

Figure 11. - Extreme cases of pop-in behavior: A, thin specimen exhibiting no well-defined pop-in; B, thick specimen where pop-in coincides with maximum load, that is, specimen breaks completely at pop-in.

of $\mathcal{G}_c$, even though a higher value could be measured by using a specimen with a longer crack, as curve B. This comparison emphasizes the point that was made earlier about the controlling significance of $\mathcal{G}_{Ic}$ in some cases, bearing in mind that test specimens are nothing more than simple examples of structural members.

Two contrasting examples of schematic R curves are shown in figure 11. Example A represents a relatively thin specimen in which the developed fracture is fully slant and the initial, triangular region of square fracture (see fig. 6(a)) (p. 9) is quite small. The magnitude of the pop-in is reduced to the point where it cannot be detected with confidence, and $\mathcal{G}_{Ic}$ cannot be measured with any confidence of accuracy. In a case like this it may be possible to obtain a well-defined pop-in measurement of $\mathcal{G}_{Ic}$ if a specimen of sufficiently greater thickness can be tested. But it should not be assumed that this will always be the case. The authors have found, by using SAE 4340 steel specimens, for instance, that well-defined pop-in's do not always occur even when specimens are used that are sufficiently thick for the developed fractures to be more than 50 percent square. This raises the question of how $\mathcal{G}_{Ic}$ might be measured for such materials, but there is no satisfactory answer to this question yet. It is hoped that research currently in progress may resolve the matter. While it is sometimes assumed that $\mathcal{G}_{Ic}$ measurements can always be satisfactorily made by testing round notched bars of sufficient size (which are discussed in the section Circumferentially Notched Round Bars), there is really no conclusive evidence at the present time that this assumption is warranted.

Example B in figure 11 represents the other extreme, in which the developed fracture of a plate specimen is almost entirely square, the pop-in is very pronounced, and the subsequent increase in R is very gradual because there is very little development of slant-fracture borders. For any practical initial crack length, the load cannot increase beyond the value at pop-in, so that $\mathcal{G}_{Ic}$ is well defined by the maximum load value and the initial crack length. The record of load as a function of crack length in this case will show a sharp peak at the load corresponding to $\mathcal{G}_{Ic}$, followed by a rapid decrease of the load.

In this section an effort has been made to describe and explain the pop-in phenomenon and its use for $\mathcal{G}_{Ic}$ measurement by reference to the Krafft hypothesis of an invariant curve of R against $a - a_o$. It is worth repeating that this hypothesis, while probably a good first approximation, may require some modification in the light of future experimental information. In fact, it will be an important aspect of fracture mechanics research in the immediate future to conduct experiments designed to test and extend this hypothesis. It seems likely that, while the dominating factor on which R depends for a given

material, thickness and testing conditions, is indeed $a - a_o$, there may well be a secondary influence of initial crack length. This might be quite significant when the initial crack length is sufficiently short so that the net section stress at $\mathcal{G}_c$ approaches the yield strength of the material. This is a situation that might be avoided in fracture mechanics testing but that is not always avoidable in practical fracture problems.

PRACTICAL SPECIMEN TYPES

The discussion has so far centered around flat tension specimens having transverse cracks of length less than one-tenth of the specimen width. These specimens are conveniently simple for the purpose of discussing general concepts. In subsequent sections various types of specimens will be considered that are more suitable for practical testing purposes, either because they require less material and lower testing load capacity, or because they provide conditions of greater elastic constraint. First, two types of specimen will be considered that are primarily intended for general $\mathcal{G}_c$ (mixed mode) toughness testing but that may sometimes be used for $\mathcal{G}_{Ic}$ measurement by the pop-in method. Then those specimen types that are regarded as suitable for $\mathcal{G}_{Ic}$ measurement only will be considered. While the specimen types discussed here are those having the most general application, there are numerous other types that have been, or could be, devised for special purposes, the only qualification being that a satisfactory specimen design must be amenable to a sufficiently accurate stress analysis to obtain an accurate expression for $\mathcal{G}$. This expression could be obtained either mathematically or experimentally, as illustrated by references 22 and 23, respectively. In particular, Winne and Wundt have discussed the use of notched rotating disks (ref. 24), and Ripling, Mostovoy, and Patrick have discussed specimens for measurement of fracture toughness of adhesive joints (ref. 25).

In connection with each of the practical specimen types the appropriate expression for $\mathcal{G}$ and the value of the effective crack length to be used in calculating $\mathcal{G}$ will be discussed, including the plastic zone correction term that is added to the observed value of the actual crack length. Also discussed will be the capacities of the various types of specimens for measurement of $\mathcal{G}_c$ or $\mathcal{G}_{Ic}$ in relation to specimen size. For this purpose, an unfamiliar symbol representing the $\mathcal{G}_c$ measurement capacity, namely, C_g is introduced to represent the maximum value of $\mathcal{G}_c$ that could be measured with acceptable accuracy with a specimen of given dimensions made of a material of given yield strength and elastic modulus. This will allow a summary comparison to be made of the different types of specimens for $\mathcal{G}_{Ic}$ testing, which indicates the merits and limitations of each type.

SYMMETRICAL PLATE SPECIMENS FOR GENERAL $\mathcal{G}_c$ MEASUREMENT

These two types of specimens are illustrated in figure 29 of appendix A (p. 55). The center-cracked type (fig. 29(a)) is provided with a simulated central transverse crack of initial length $2a_o$ equal to about 0.3 W, where W is the width and is obviously a modification of the wide plate specimen having a longer crack for a given width. The symmetrically edge-cracked type

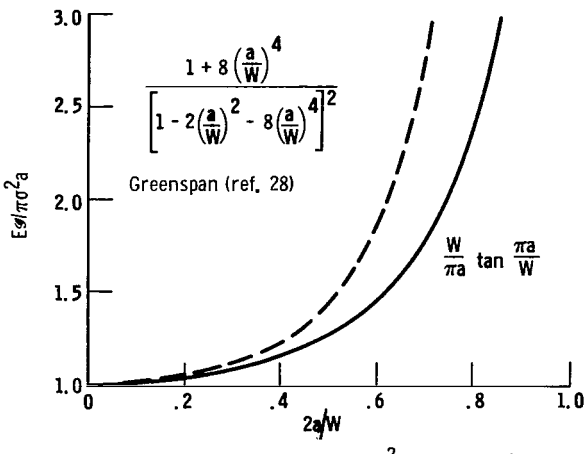

Figure 12. - Comparison of $E\mathcal{G}/\pi\sigma^2 a$ against 2a/W according to Greenspan and tangent expressions for symmetrically center-cracked plate specimens showing that difference is not inconsequential.

(fig. 29(b) (p. 55)) is provided with equal transverse edge cracks of initial length a_o equal to about 0.15 W. These two specimens are essentially equivalent except for a slight difference in the expressions for $\mathcal{G}$, and the choice between them is mainly a matter of convenience in preparation. The discussion will therefore be confined largely to the center-cracked specimen with the understanding that it applies in general equally to the symmetrically edge-cracked specimen.

The elastic strain energy field in the vicinity of the ends of the crack is appreciably influenced by the proximity to the free edges of the specimen when 2a/W exceeds about 0.1. Consequently, $\mathcal{G}$ is then no longer given with sufficient accuracy by the equation $E\mathcal{G} = \pi\sigma^2 a$. The appropriate expression recommended by the ASTM Special Committee on Fracture Testing (ref. 5) is the tangent form derived by Irwin (refs. 11 and 17) from an analysis by Westergaard (ref. 26): $E\mathcal{G} = \sigma^2 W \tan(\pi a/W)$. An earlier expression was derived by Kies (ref. 27) from the work of Greenspan (ref. 28) and is known as the Greenspan or polynomial form. While this form is occasionally still used, it is preferable to use the tangent form in the interests of consistency with the majority of investigators. To show that the difference between these expressions is not inconsequential, they are compared in figure 12 on a dimensionless basis, $E\mathcal{G}/\pi\sigma^2 a$, which is equal to the configurational or geometric factor in each case plotted against 2a/W.

Effective Crack Length and Plastic Zone Correction Term

The value of the effective crack length 2a, which should be used in calculating $\mathcal{G}$ from the tangent equation given previously, is not simply the estimated average length of the actual crack at instability $2a_m$, but also includes a term $2r_Y$ to correct for the stress-relaxing effect of the plastically deformed zones at each end of the crack; that is, $a = a_m + r_Y$. When a state of generalized plane stress is assumed, as in the case of a $\mathcal{G}_c$ measurement at ultimate instability, r_Y is taken to be equal to $E\mathcal{G}/2\pi\sigma_{YS}^2$, where σ_{YS} is the 0.2 percent offset tensile yield strength. For a state of plane strain, usually assumed for $\mathcal{G}_{Ic}$ measurements, r_{IY} may be taken as one-third of the plane stress value, that is, $E\mathcal{G}/6\pi\sigma_{YS}^2$. The basis for these correction terms has been thoroughly discussed in the literature (refs. 5, 11, and 29) so that no extensive discussion is needed here. It is important here, however, to emphasize the point that this method of correcting an assumed elastic stress analysis to take account of inelastic strain in a limited region is somewhat arbitrary and approximate. For this reason, calculated values of $\mathcal{G}$ should be regarded as increasingly inaccurate the greater the ratio r_Y/a. This is one factor that should be considered in deciding how large a specimen is needed

for an accurate measurement of $\mathcal{G}_c$, but the basis of the current recommendation of the ASTM Special Committee on Fracture Testing on this point is somewhat different, as discussed in the following section.

The calculation of $\mathcal{G}$ is complicated by the inclusion of the plastic zone correction term, which itself is a function of $\mathcal{G}$. Except in the simplest case of the wide plate specimen, $\mathcal{G}$ cannot be expressed as an explicit function of the load and the specimen dimensions and must be calculated from the implicit equation by either a graphical or an iteration procedure. The graphical procedure for the symmetrically cracked plate specimens is described in reference 5. The iteration procedure is simply a matter of first calculating a first approximation to $\mathcal{G}$ by neglecting r_Y, next calculating a second approximation to $\mathcal{G}$ entailing a value of r_Y based on the first approximation to $\mathcal{G}$, and so on. Convergence will normally be very rapid, and the iteration procedure is the natural one to use for a digital computer calculation program.

$\mathcal{G}_c$ Measurement Capacity in Relation to Specimen Size

If the width of a center-cracked plate specimen is less than some value that is directly proportional to the value of $\mathcal{G}_c$ to be measured, the average net section stress at instability will exceed the uniaxial tensile yield strength of the material. A test of this sort is not represented even approximately by a linear elastic stress field model and therefore does not provide a useful measurement of $\mathcal{G}_c$. Even when instability occurs at an average net section stress less than the yield strength, the accuracy of $\mathcal{G}_c$ measurement is lower the greater the value of r_Y/a, as mentioned earlier. The ratio r_Y/a increases in proportion to the square of the ratio of the average net section stress to the yield strength for a given value of $2a/W$. It follows that the larger the specimen that is tested, the more accurate the measurement of $\mathcal{G}_c$ is likely to be. Similar considerations apply to the specimens for $\mathcal{G}_{Ic}$ testing, which will be discussed in the section SPECIMENS SUITABLE FOR $\mathcal{G}_{Ic}$ MEASUREMENT ONLY.

It is of considerable practical importance to be able to estimate how large a value of $\mathcal{G}_c$ could be measured with acceptable accuracy by using a center-cracked specimen of a given width W. For this purpose the ASTM Special Committee on Fracture Testing has suggested the criterion that the $\mathcal{G}_c$ measurement will be sufficiently accurate if the average net section stress at instability does not exceed 80 percent of the 0.2 percent offset tensile yield strength, σ_{YS} (ref. 9). This is a tentative recommendation based on a limited number of tests of specimens having different widths and crack lengths, which indicated that $\mathcal{G}_c$ was independent of width and crack length when this condition was satisfied. It would appear that the materials used for these tests must have R curves of a type that would result in $\mathcal{G}_c$ being insensitive to crack length, that is, like type A in figure 2 (p. 7) rather than types B or C. It should be noted that there is a distinction to be made here between an intrinsic dependence of $\mathcal{G}_c$ on crack length due to the shape of the R curve, which exists even when the test is well represented by the linear elastic stress field model, and an apparent dependence of $\mathcal{G}_c$ on crack length that occurs when the average stress is too close to yield to be properly represented by the linear elastic model.

Substituting the condition $\sigma_{net} = 0.8\ \sigma_{YS}$ in the tangent equation yields for C_g the maximum value of $\mathcal{G}_c$ that could be measured with acceptable accuracy for a given yield strength, elastic modulus, and specimen dimensions

$$C_g = 0.64\ \frac{\sigma_{YS}^2}{E}\ W\left(\frac{1 - 2a_m}{W}\right)^2 \tan\ \frac{\pi a}{W}$$

where a_m is the estimated average half-length of the actual crack at instability, and $a = a_m + r_Y$.

This expression for C_g can be regarded as the product of four distinct factors, each having a particular significance:

(1) The numerical constant 0.64 represents a factor of utilization based on experimental results.

(2) The dependence of C_g on the properties of the material under test is represented by σ_{YS}^2/E.

(3) The width W is the characteristic dimension representing specimen size.

(4) The effect of the ratio of crack length to width is represented by a dimensionless factor $(1 - 2a_m/W)^2 \tan(\pi a/W)$.

The length of the specimen should be proportional to W and chosen to be sufficient so that there is a region of uniform stress distribution between the crack and each of the end regions of the specimen through which the load is applied. Photoelastic studies have confirmed that the proportions of the specimens shown in figure 29 (p. 55) of appendix A are just about sufficient for the pin-loading method shown. With proportionately shorter specimens, the interference between the stress field of the crack and that of each of the loading pin holes would be appreciable. Specimen thickness for $\mathcal{G}_c$ measurement may be varied over a considerable range for a given value of W, as indicated in figure 29, and will be discussed in the next section.

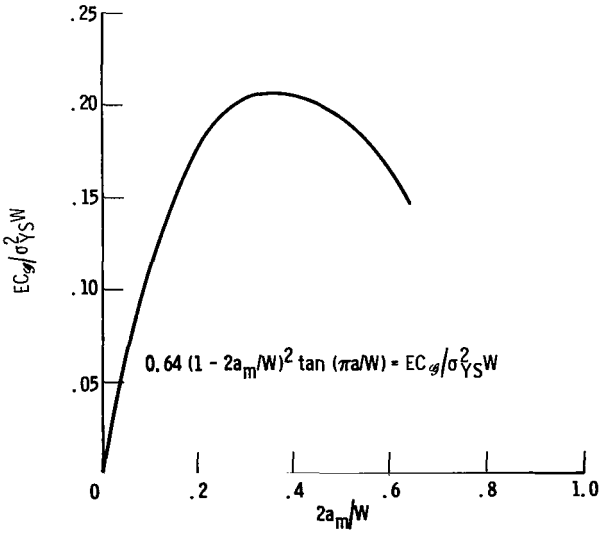

Figure 13. - Dependence of EC_g/σ_{YS}^2W for symmetrically center-cracked specimens on $2a_m/W$, where C_g is estimate of maximum value of $\mathcal{G}_c$ that can be measured with acceptable accuracy for given values of W, E, and σ_{YS} (see text).

From the expression for C_g given previously it follows that the most efficient value of $2a_m/W$ will be that for which the quantity $0.64(1 - 2a_m/W)^2 \tan(\pi a/W)$, which is equal to EC_g/σ_{YS}^2W, is greatest. This quantity is plotted against $2a_m/W$ in figure 13, showing that the maximum

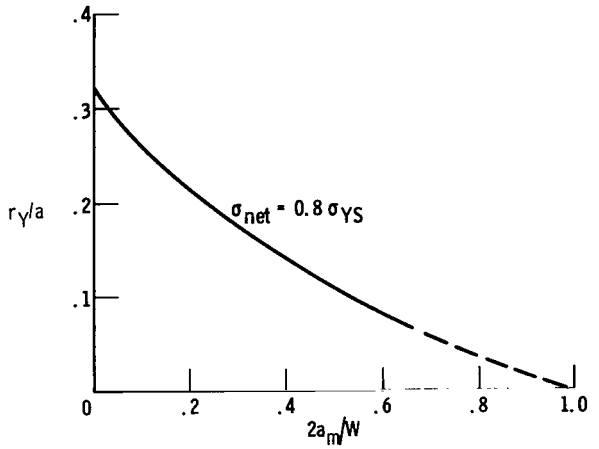

Figure 14. - Ratio of plastic zone size correction term to effective crack half-length r_Y/a against $2a_m/W$ at limiting condition for use of center-cracked plate specimens for $\mathcal{G}_c$ measurement, $\sigma_{net} = 0.8\,\sigma_{YS}$.

occurs in the range of $2a_m/W$ between 0.3 and 0.4. This is the basis for the recommendation that $2a_o$ should be about 0.3 W for the center-cracked specimen. The useful range of $2a_m/W$ extends up to about 0.6; beyond this point, the accuracy of the expression for $\mathcal{G}$ becomes increasingly dubious (ref. 11). Furthermore, the accuracy of the estimate of $\mathcal{G}$ becomes increasingly dependent on the accuracy of the value of a that is used, and this is the least accurate of the several measurements from which $\mathcal{G}$ is calculated. Thus, if $2a_m/W$ exceeds 0.6 in any test, the result should not be used for anything more than a rough estimate of $\mathcal{G}_c$. Additional tests of wider specimens are necessary for accurate $\mathcal{G}_c$ measurement in such cases.

For values of $2a_m/W$ much less than 0.3, limitation of the average net section stress to 80 percent of the yield strength may not be a sufficient indication that an acceptably accurate determination of $\mathcal{G}_c$ will result. The reason is that, for $\sigma_{net} = 0.8\,\sigma_{YS}$, the ratio r_Y/a increases as $2a_m/W$ increases, as shown in figure 14. To a first approximation, if the estimate of r_Y as $E\mathcal{G}/2\pi\sigma_{YS}^2$ is in error, the consequent error in the calculated value of $\mathcal{G}$ will be proportional to r_Y/a multiplied by the error in r_Y. In reference 30 it is suggested that the value of r_Y is unlikely to differ from the estimate of $E\mathcal{G}/2\pi\sigma_{YS}^2$ by more than about ±25 percent, so that the consequent error in the calculated value of $\mathcal{G}$ would be expected to be no greater than $25r_Y/a$ percent. The value of this limit increases from 4.4 percent at $2a_m/W$ equal to 0.3, to 8 percent as $2a_m/W$ approaches zero (from fig. 14). In general, it would seem desirable that r_Y/a should not exceed about 0.2, so that any associated error in $\mathcal{G}$ would be likely to be less than 5 percent.

The $\mathcal{G}_c$ measurement capacity of a center-cracked specimen C_g may be estimated by referring to figure 13. The value of the ordinate for a given value of $2a_m/W$ is equal to the value of $EC_g/\sigma_{YS}^2 W$. When $2a_m/W$ is between 0.3 and 0.45, C_g is slightly greater than $0.2\,W\sigma_{YS}^2/E$, and this value may be regarded as the maximum $\mathcal{G}_c$ measurement capacity of the center-cracked type of specimen. The maximum K_c measurement capacity is therefore about $0.45\,\sigma_{YS}W^{1/2}$. The same figures can be used in estimating the toughness measurement capacities of symmetrically edge-cracked specimens.

Variation of $\mathcal{G}_c$ with Crack Length and Specimen Width

The preceding discussion of $\mathcal{G}_c$ measurement capacity involved the im-

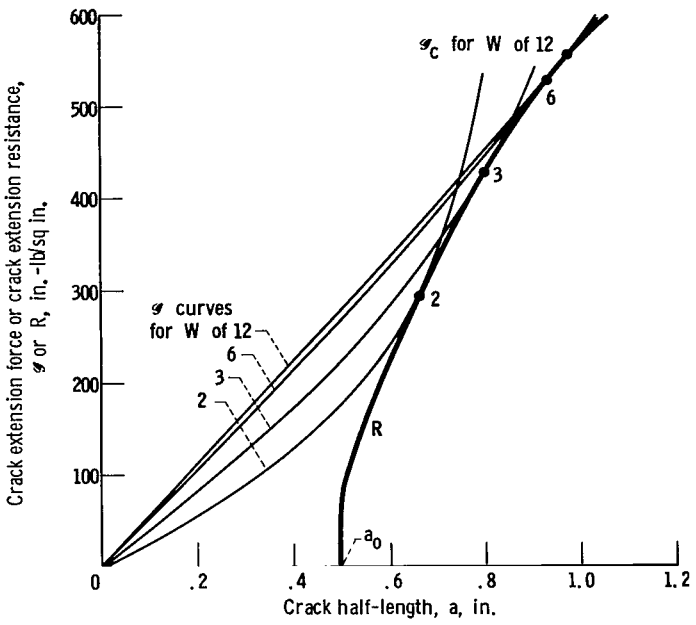

Figure 15. - Showing dependence of $\mathcal{G}_c$ on specimen width W for center-cracked plate specimens having same initial crack half-length a_o of material having an R curve identical to that of figure 4 except for difference of scale.

plicit assumption that $\mathcal{G}_c$ would be independent of initial crack length, as would be the case for a material with an R curve similar to type A in figure 2 (p. 7). Assuming $\mathcal{G}_c$ to be independent of initial crack length enabled avoidance of an unduly complicated discussion of $\mathcal{G}_c$ measurement capacity, and the conclusions reached are not substantially different from those that would have followed from a more general discussion.

The next question to be discussed is how $\mathcal{G}_c$ might depend on crack length and specimen width in the case of a material having a different kind of R curve, for instance, type B of figure 2. This question was discussed earlier with reference to center-cracked plate specimens for which $2a/W$ was less than 0.1 (fig. 4, p. 8). The discussion will now consider specimens for which $2a/W$ is greater than 0.1.

Figure 15 shows an R curve that is identical to those in figure 4 apart from scale. The particular $\mathcal{G}$ traces that are tangent to the R curve for specimens of widths 2, 3, 6, and 12 inches are also shown, the initial crack length being 1 inch in each case. These $\mathcal{G}$ traces are no longer straight lines, as in figure 4, but are constructed from the equation $E\mathcal{G} = \sigma^2 W \tan(\pi a/W)$, the appropriate values of σ required to satisfy the tangency condition being obtained by graphical interpolation. As discussed in the earlier section on "Crack Extension Resistance and the Occurrence of Instability," the points of tangency represent the values of $\mathcal{G}_c$ that would be measured according to our criterion of instability. The main point of figure 15 is that, for a given initial crack length and an R curve of this type, the measured value of $\mathcal{G}_c$ decreases as the specimen width is decreased. Furthermore, the dependence of $\mathcal{G}_c$ on W is stronger the larger the value of $2a_o/W$. These conclusions are, of course, drawn from a construction on the basis of the hypothesis that R is a function of $a - a_o$ only (ref. 12). The results given in reference 12 for aluminum 7075.T6 are generally consistent with figure 15, the R curve in that figure having been obtained from those results, but the agreement between measured and predicted values of $\mathcal{G}_c$ is no more than fair. This simply means that more extensive experimental investigation of the hypothesis is needed, the fact that $\mathcal{G}_c$ may depend on specimen width in the manner shown by figure 15 is not in question. The degree of the dependence, however, will be determined by the material, its thickness, and testing speed and temperature, and may be imperceptible in some cases.

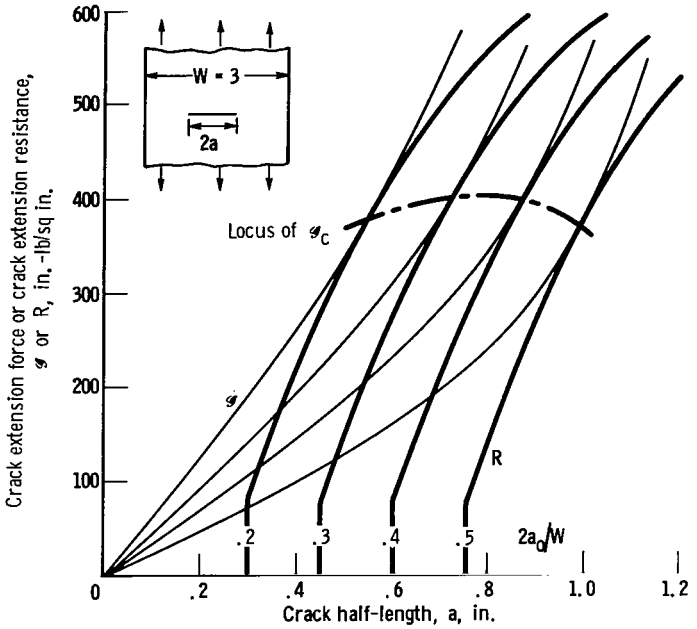

Figure 16. - Showing dependence of $\mathcal{G}_c$ on relative initial crack length $2a_o/W$ for center-cracked plate specimens of initial width W = 3 inches of material having an R curve identical to that of figures 4 and 15.

Figure 16 shows the predicted dependence of $\mathcal{G}_c$ on $2a_o/W$ for a fixed specimen width of 3 inches when the R curve is identical with that of figure 15. The value of $\mathcal{G}_c$ does not vary greatly over the range of $2a_o/W$ between 0.2 and 0.5, and the locus has a maximum at $2a_o/W$ equal to about 0.35. The contrast between this figure and figures 4 and 15 is rather surprising. The explanation is that $\mathcal{G}_c$ increases with increasing crack length, as in figure 4, but decreases as $2a_o/W$ increases for a given value of the initial crack length, as in figure 15. These two effects oppose one another when the specimen width is kept constant and the crack length varied, as in figure 16. The crack length effect dominates for the smaller values of $2a_o/W$, resulting in an initial increasing trend of $\mathcal{G}_c$ with $2a_o/W$. For values of $2a_o/W$ greater than about 0.35, however, the effect of the restricted specimen width dominates and the trend is reversed. Of course, this is just one example, and it is to be expected that the form of the $\mathcal{G}$ locus will vary with the form of the R curve, but the opposing effects will exist to some degree in any case. Perhaps the most important point to be made is that it is possible to obtain a false impression of the degree of independence of $\mathcal{G}_c$ from a series of tests in which the specimen width is kept constant and the initial crack length is varied.

Since the measured value of $\mathcal{G}_c$ will depend on both initial crack length and specimen width to a greater or lesser degree, determined by the form of the R curve for the material and thickness under investigation, there is some question as to how particular $\mathcal{G}_c$ measurements are to be used. This question cannot be satisfactorily answered until the R curves of a sufficient variety of materials have been determined and evaluated in sufficient detail. At the present time it would seem only prudent to evaluate $\mathcal{G}_c$ for several crack lengths in the case of any material and thickness that is intended to be used in a particular application.

As far as evaluating the fracture toughness of materials, in general, is concerned, $\mathcal{G}_{Ic}$ is apparently independent of any specimen dimension and thus provides an invariant fracture characteristic for many of the materials of engineering interest. This is the main reason why effort on $\mathcal{G}_{Ic}$ testing has increased in recent years at the expense of effort on $\mathcal{G}_c$ testing.

It is not to be concluded, however, that $\mathcal{G}_c$ testing should be abandoned

in favor of $\mathcal{G}_{Ic}$ testing exclusively. Rather, $\mathcal{G}_c$ tests should be conducted primarily in relation to specific structural components and should be conducted in sufficient detail that the $\mathcal{G}_c$ values determined are relevant to circumstances of failure that are pertinent to the component in question. For example, in an airplane skin, tolerance for a crack several inches long is desirable, if not mandatory, but in a rocket casing, it may be necessary to use materials that cannot tolerate cracks that are only a fraction of an inch long. These different cases call for different approaches to $\mathcal{G}_c$ testing. Material selection in relation to risk of fracture should entail at least two stages. The first, screening stage would utilize a standardized specimen appropriate to the application and would serve to reduce the number of candidate materials to a preferred few. These would then be subjected to more extensive testing involving a range of crack sizes, perhaps even to determination of the entire R curve for the thickness of interest. What is most important is that it should be appreciated that neither the planning nor the interpretation of $\mathcal{G}_c$ tests is a routine matter.

The question of specimen thickness should be discussed to conclude the subject of $\mathcal{G}_c$ testing before taking up $\mathcal{G}_{Ic}$ testing. This will lead naturally into a general discussion of $\mathcal{G}_{Ic}$ measurement and then to consideration of other types of specimen for this purpose.

Thickness of Symmetrical Plate Specimens

The ASTM Special Committee on Fracture Testing has recommended that the specimen thickness B for fixed mode or slant mode $\mathcal{G}_c$ measurement should be between $W/45$ and $W/16$, except that the lower limit need not apply if proper measures are taken to prevent buckling around the crack when B is less than $W/45$ (ref. 5). In the experience of one of the authors, buckling of symmetrically edge-cracked specimens is less apt to occur than is the case with center-cracked specimens. In any case, supporting the specimen between lubricated face plates is an effective method of preventing buckling of thin specimens and ensuring that accuracy of $\mathcal{G}_c$ measurement is not impaired thereby.

The restriction that B should not exceed $W/16$ applies only when it is desired to measure $\mathcal{G}_c$, as distinct from $\mathcal{G}_{Ic}$ by the pop-in method. It has to do with the change in crack front configuration as the crack extends from the initial fatigue crack front, which is nearly square and straight, in the stable range preceding instability. It is useful at this point to refer to figure 6 (p. 9). With the assumption that the crack will eventually develop into the slant type (the most extreme case), the distance over which the development takes place will be roughly proportional to B, and of about equal magnitude (fig. 6(a)). For $2a_o/W$ equal to about 0.3 and B not greater than $W/16$, development of full slant fracture should be completed at some value of $2a_m/W$ less than 0.6. For greater thicknesses there is a possibility that development of full slant fracture may not be complete when $2a_m/W$ equals 0.6, and instability might occur at some value of $\mathcal{G}$ lower than that appropriate to the thickness and width. While no specific data are available on this point, general experience indicates that there is good reason to respect this restriction.

For materials of such thickness that the specimen will exhibit a predominantly square fracture the restriction could be less severe, as implied in reference 5. For $\mathcal{G}_{Ic}$ measurements, there appears to be no basic reason to impose any upper limit on the thickness, but there is an optimum value of the ratio B/W.

In their original study of the pop-in method of $\mathcal{G}_{Ic}$ measurement, Boyle, et al. (ref. 21) observed distinct pop-in indications with aluminum 7075.T6 specimens that had thicknesses no less than $2E\mathcal{G}_{Ic}/\pi\sigma_{YS}^2$, that is, not less than four times the value of r_Y corresponding to $\mathcal{G}_{Ic}$. Distinct pop-in indications were not observed with specimens that were thinner than this. The qualitative explanation of these observations is that, when the plane stress plastic zone size approaches one-half the specimen thickness, the component of stress in the thickness direction will be relaxed along the major part of the crack front so that a state of plane strain no longer prevails. It is to be expected that the limiting value of the ratio r_Y/B for distinct pop-in detection would differ somewhat from one material to another, but in the absence of any additional information the conclusion from reference 21 will be used, namely, that B should not be less than $2E\mathcal{G}_{Ic}/\pi\sigma_{YS}^2$, as a necessary condition for a satisfactory pop-in $\mathcal{G}_{Ic}$ measurement. It should be appreciated, however, that it is not necessarily also a sufficient condition in all cases. As mentioned earlier, it appears that some materials may not exhibit any distinct $\mathcal{G}_{Ic}$ metainstability.

In reference 21 it is also suggested that the specimen width for $\mathcal{G}_{Ic}$ measurements can be as small as $10E\mathcal{G}_{Ic}/\pi\sigma_{YS}^2$. This corresponds to a restriction of the average net section stress to be less than the yield strength, rather than less than 80 percent of the yield strength as recommended by the ASTM Special Committee on Fracture Testing for $\mathcal{G}_c$ measurements. Until more data become available to support the less restrictive estimate of reference 21, it appears advisable to adhere to the recommendation of the ASTM Committee for $\mathcal{G}_{Ic}$ pop-in measurement as well as for $\mathcal{G}_c$ testing.

From these considerations, it appears that the optimum range of B/W for symmetrically cracked plate specimens used for pop-in $\mathcal{G}_{Ic}$ measurement is between 1/5 and 1/10. This does not mean that specimens of width greater than 10B should not be used when it is convenient to do so, only that the $\mathcal{G}_{Ic}$ measurement capacity in that case will be limited by the thickness, not by the width. Also, specimens having W less than 5B could be used, but when the available form of the material to be tested makes this desirable, it is both more convenient and more efficient to use single-edge-notched specimens, loaded either in tension or bending, as will be discussed in subsequent sections. With one exception, it will be assumed that the $\mathcal{G}_{Ic}$ measurement capacities of all types of plate specimens are limited to the same extent by thickness, namely, $C_{Ig} = \pi\sigma_{YS}^2 B/2E$, according to the preceding discussion. The exception is the surface cracked type of plate specimen in which the crack propagates initially in the thickness direction of the specimen, not in the width direction as in the other types.

Plane Strain Plastic Zone Correction Term - $\mathcal{G}_{Ic}$ and K_{Ic} Calculations

Before considering the other types of specimens that are intended for plane strain crack toughness testing, there are two general points that are relevant to all such tests. First, in calculating values of $\mathcal{G}_{Ic}$, a plastic zone correction term may be added to the estimated average value of the actual crack length, just as in the case of $\mathcal{G}_c$ calculations. There are two differences, however: (1) It is assumed that no stable crack extension occurs, and the initial crack length is used in the calculation. (2) The plane strain plastic zone correction term is taken to be one-third of the plane stress term, that is, $r_{IY} = r_Y/3 = E\mathcal{G}_{Ic}/6\pi\sigma_{YS}^2$ (refs. 21 and 29). Very often this term can be neglected entirely without significantly affecting the accuracy of the $\mathcal{G}_{Ic}$ measurement. When it is taken into account, the $\mathcal{G}_{Ic}$ calculation is most readily carried out by the aforementioned iteration procedure. Usually, only one iteration is necessary.

The other point concerns the relation between K_{Ic} and $\mathcal{G}_{Ic}$. As mentioned earlier, for plane strain conditions: $K_I^2 = E\mathcal{G}_I/(1 - \nu^2)$. For pop-in $\mathcal{G}_{Ic}$ tests, however, there is an unresolved problem of the degree to which the stress field in the vicinity of the middle of the crack front approaches a state of plane strain (ref. 23). As in reference 21, it is usual to calculate K_{Ic} from the plane strain relation given previously simply because there is no basis at present for estimating the degree to which the stress state deviates from the plane strain state. The possible error in the calculated value of K_{Ic} resulting from this assumption could not exceed about 5 percent and is probably much less.

SPECIMEN TYPES SUITABLE FOR $\mathcal{G}_{Ic}$ MEASUREMENT ONLY

The types of specimens in this category that will be discussed are illustrated in figure 30 (p. 56) of appendix A as follows:

(a) Single-edge-notched plate specimen loaded in tension

(b) Notched rectangular-section bend specimen, three-point loading

(c) Notched rectangular-section bend specimen, four-point loading

(d) Surface cracked (or part-through cracked) plate specimen

(e) Circumferentially notched round bar specimen

While these specimens are referred to for brevity as notched specimens, it is to be understood that the notches should always terminate in sharp cracks, usually provided by fatigue stressing.

Single-Edge-Notched Tension Specimens

This type of specimen was first introduced for the purpose of plane strain crack toughness measurement by Irwin, Krafft, and Sullivan in an unpublished memorandum to the ASTM Special Committee on Fracture Testing in August 1962. Subsequently, Sullivan published a discussion of the particular design of single-edge-notched specimen used by these investigators (ref. 30).

A single-edge-notched tension specimen can be regarded as derived from either type of symmetrically cracked plate specimen, bisected along the longitudinal centerline and shortened accordingly. Since this operation affects neither the thickness nor the simulated crack size (a_o remains the same), it might be expected that the $\mathcal{G}_{Ic}$ measurement capacity of each half would be about the same as that of the symmetrical specimen from which it was derived. If this were the case, the amount of material required for a single-edge-notched specimen of given $\mathcal{G}_{Ic}$ measurement capacity would be only one-fourth of the amount required for a symmetrically cracked specimen of equal capacity with the assumption of the same ratio of length to width for the two types of specimens. Actually, the size advantage of the single-edge-notched specimen is probably not nearly this great, but it does have another advantage in requiring considerably less load to determine a given $\mathcal{G}_{Ic}$ value than does a symmetrically cracked specimen. This could be a determining factor in the choice of specimen type when it is necessary to test very large specimens of materials having high ratios of toughness to yield strength.

Up to the present time, no expression for $\mathcal{G}$ in closed form has been derived for single-edge-notched tension specimens. Approximate expressions of very good accuracy have been obtained, however, by a mathematical procedure of boundary collocation applied to a suitable stress function (ref. 22) and by the experimental compliance measurement procedure (ref. 23). The experimental method was originally suggested by Irwin and Kies (ref. 31), and, in principle, is of general utility. The expression for $\mathcal{G}_{Ic}$ given in figure 30(a) (p. 56) is taken from reference 23 and applies strictly for the given values of D/W and L/W, where D is the distance of the axis of loading from the cracked edge of the specimen and L is the distance between loading pin holes. In figure 30(a) D/W is $1/2$, and L/W is $8/3$.

It is convenient to express the results of collocation computations or of experimental compliance measurements in the form of dimensionless factors that are functions of $\mathcal{G}$, the applied load P, and the pertinent specimen dimensions. In the case of single-edge-notched tension specimens for given values of the ratios D/W and L/W, the appropriate dimensionless factor is $E\mathcal{G}B^2W/P^2$, which depends only on a/W. In other words, if the proportions of the specimen dimensions other than thickness are kept constant, the value of $E\mathcal{G}B^2W/P^2$ for a given value of a/W will be the same regardless of the size of the specimen, its thickness, or the material from which it is made. This factor can therefore be expressed universally as a function of a/W in the form of a table, a curve, or a suitable polynomial in a/W obtained by least-squares best-fit procedures applied to the tabulated results. The polynomial form is a convenient way to express the relation between $E\mathcal{G}B^2W/P^2$ and a/W compactly, as in appendix A. Experience has shown that a third-degree poly-

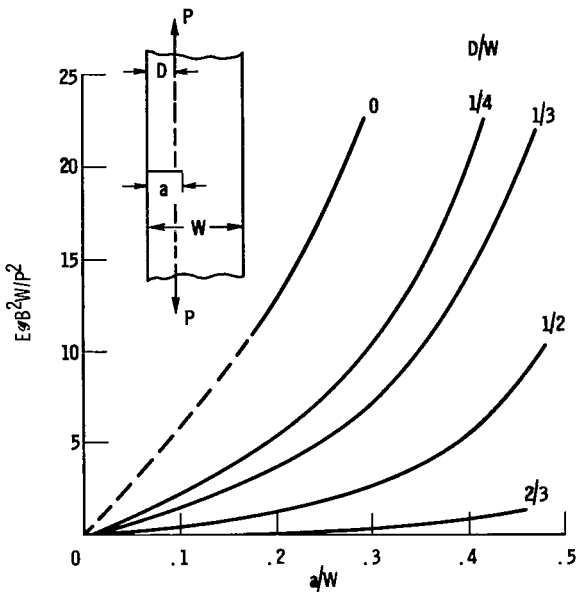

Figure 17. - Dependence of relation between dimensionless calibration factor $E\mathcal{G}B^2W/P^2$ and a/W for single-edge-notched tension specimens on location of axis of loading as specified by parameter D/W.

nomial is sufficient to provide an adequate fit, as discussed in more detail in reference 23.

The ratios L/W and D/W are additional parameters that cannot be combined with $E\mathcal{G}B^2W/P^2$ into a more general dimensionless factor in any simple way for the single-edge-notched tension specimen. (It will be shown later, however, that a rather more general dimensionless factor can be devised for bend specimens.) Providing L/W is sufficiently large, the effect of small variations of L/W on $E\mathcal{G}B^2W/P^2$ is negligible, and the expression for $E\mathcal{G}_{Ic}B^2W/P^2$ given in figure 30(a) can be used with confidence provided that L/W is held to 8/3 within 5 percent. If circumstances make it necessary to use a shorter specimen, such as that described in reference 30, an experimental calibration should be conducted for the specific specimen proportions to be used. In this case it would be advisable to read the discussions relating to specimen length given in references 22 and 23.

The value of $E\mathcal{G}B^2W/P^2$ for a given value of a/W depends very strongly on D/W, as shown in figure 17. The curves for various values of D/W are derived from unpublished work by B. Gross of Lewis, who used the boundary collocation procedure mentioned earlier. The figure is intended to be illustrative only, not for calculation purposes. Mainly, the figure indicates that once a value of D/W has been decided on and an accurate expression for $E\mathcal{G}B^2W/P^2$ against a/W obtained for that value of D/W, it should be held within close tolerances in order to avoid errors that would result from deviations from the nominal value.

There is actually no good reason to choose a value of D/W different from 1/2, for which an expression for $E\mathcal{G}B^2W/P^2$ of adequate accuracy already exists (fig. 30(a) and refs. 22 and 23). It is true that the load required to measure a given value of $\mathcal{G}_{Ic}$ will be lower the smaller is D/W, but this load could be reduced even more by using a bend specimen instead of loading in tension. On the other hand, the sensitivity of $\mathcal{G}$ to a small error in the measured value of a_o is greater the smaller is D/W, so that $\mathcal{G}_{Ic}$ measurement accuracy decreases as D/W is decreased. It would seem that having a choice between a bend specimen (requiring lower load) and a single-edge-notched tension specimen with D/W equal to 1/2 (providing better accuracy) would be sufficient without complicating the issue by considering tension specimens having other values of D/W.

Now that the essential features of the design of single-edge-notched ten-

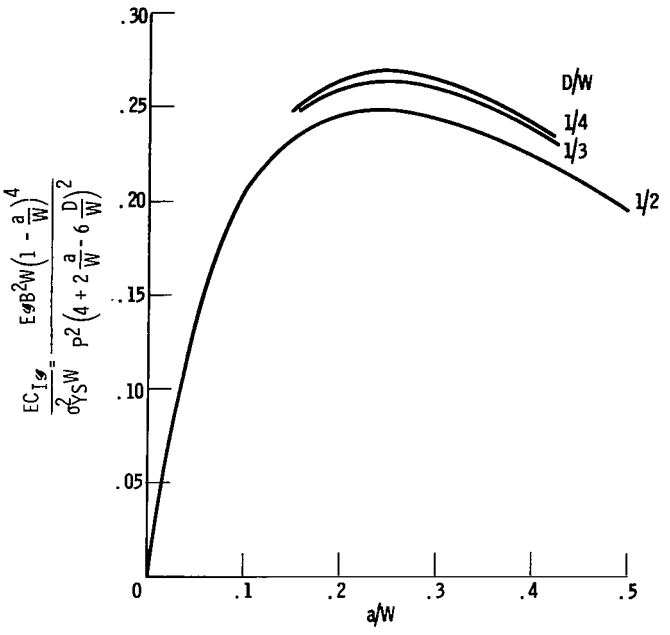

Figure 18. - Dependence of $EC_{I\mathcal{G}}/\sigma_{YS}^2 W$ for single-edge-notched tension specimens on a/W for three values of D/W, which specifies location of loading axis, as in figure 17.

sion specimens have been discussed, the $\mathcal{G}_{Ic}$ measurement capacity of this type can be considered. The criterion used for this purpose is that the nominal stress at the crack tip should not exceed the yield strength. This is admittedly somewhat arbitrary, but is analogous to the criterion discussed previously for the symmetrically cracked specimens, except that the maximum value of the average net section stress was limited to $0.8\ \sigma_{YS}$ in that case. For the single-edge-notched specimen, the decrease of nominal stress with distance from the crack tip is the justification for using a somewhat higher limit for the nominal stress at the crack tip.

What is meant by the nominal stress at the crack tip is the tensile stress that would exist at the edge of a strip of width W - a under an eccentric tensile load P acting at a distance D - a from that edge, obviously derived from a single-edge-notched specimen by removing a longitudinal strip containing the notch without changing the position of the loading axis. The stress is given by the relation

$$\sigma_{nom} = \frac{P}{B(W - a)} + \frac{3P(W + a - 2D)}{B(W - a)^2}$$

From this relation and the results from which figure 17 was plotted, the values of $E\mathcal{G}/\sigma_{YS}^2 W$ that correspond to $\sigma_{nom} = \sigma_{YS}$ can be formally calculated. The three curves shown in figure 18 for values of D/W of 1/4, 1/3, and 1/2 are plotted from the results of such calculations. These curves represent the dependence of the quantity $EC_{Ig}/\sigma_{YS}^2 W$ on a/W for the three different D/W ratios, and have the same significance as the curve shown in figure 13 for the center-cracked specimen (with the assumption that the respective criteria on which they are based are equivalent). The shapes and relative positions of the three curves in figure 18 would not be changed by taking the ratio σ_{nom}/σ_{YS} as having some value different from unity. Only the ordinate scale would be changed in proportion to the square of this ratio; therefore, the figure shows two things. First, that the maximum efficiency depends very little on D/W, being somewhat higher the lower the value of D/W. The slight advantage in efficiency when D/W is low is unlikely to be worth the decrease in accuracy of $\mathcal{G}_{Ic}$ measurement. Secondly, regardless of the value of D/W, the efficiency is greatest when a/W is about 0.25, but varies only about 5 percent in the range of a/W between 0.15 and 0.35.

With the assumption that the $\mathcal{G}_{Ic}$ measurement capacities of the center-cracked specimen type and the single-edge-notched tension specimen type are reasonably well represented by figures 13 and 18, respectively, it is apparent that the single-edge-notched type has only a marginally greater capacity for a given width than the center-cracked type. Thus, it would appear erroneous to make the simple assumption that bisecting a symmetrically cracked specimen would result in two single-edge-notched specimens each having the same $\mathcal{G}_{Ic}$ measurement capacity as the symmetrically cracked specimen. Actually, the analysis just presented is open to question, and it will probably require considerable experimental work to arrive at good estimates of the $\mathcal{G}_{Ic}$ measurement capacities of the various types of specimens. In the interim, in order to have some basis for deciding on specimen dimensions, this analysis and similar analyses that appear to be predicated upon reasonable assumptions will be used.

There is no reason to suppose that the limitation imposed by thickness would be different for the single-edge-notched type than for the center-cracked type of specimen. Hence, it is deduced that the optimum range of B/W for the single-edge-notched type should be about 1/4 to 1/8 in contrast to 1/5 to 1/10, derived earlier for the center-cracked type.

Notched Bend Specimens

The notched rectangular-section bend specimen was one of the earliest types of specimen to be used for fracture toughness testing. It was not at first appreciated that it was necessary to provide a notch that terminated in an actual crack, nor that the specimen, while suitable for $\mathcal{G}_{Ic}$ testing by pop-in measurement, was not suitable for accurate $\mathcal{G}_{c}$ testing under circumstances where the fracture was not predominantly square. Consequently, much of the early data obtained with notched bend bars is only useful in a semiquantitative sense.

There is no essential distinction between a notched rectangular-section bend specimen and a single-edge-notched plate specimen tested in tension. The notched rectangular-section bend specimen is simply the extreme case of the single-edge-notched plate specimen when the loading results from a couple without any additional tension component. For one of several practical reasons, it may be more convenient to test specimens in bending rather than in tension, and, in particular, the load needed to measure a given value of $\mathcal{G}_{Ic}$ is less for a bend specimen than for any other type. On the other hand, it is to be expected that the accuracy of $\mathcal{G}_{Ic}$ measurement is inherently lower for the bend specimen than for any other type because the sensitivity of the calculated value of $\mathcal{G}$ to a small error in a_o is greater than for any other type.

Recommended dimensions for bend specimens are shown in figure 30(b) and (c) (p. 56). The symbol W is used for the beam depth because this dimension corresponds with the width of a single-edge-notched tension specimen. The beam thickness is B, and L is the moment arm length, that is, half the difference between the major and the minor spans, which reduces to half the span for three-point loading. The total applied load P is assumed to be equally distributed. The bending moment within the minor span is therefore PL/2.

The most general dimensionless factor that can be used to express $\mathcal{G}$ as a function of a/W for a bend specimen is $E\mathcal{G}B^2W^3/P^2L^2$, that is, W^2/L^2 times the less general factor $E\mathcal{G}B^2W/P^2$, which was used for the single-edge-notched tension specimen. This simply takes into account the fact that $E\mathcal{G}B^2W/P^2$ is proportional to L^2/W^2 for bend specimens having a given value of a/W. This was deduced originally by G. R. Irwin in an unpublished note and later confirmed by a different method by B. Gross of Lewis (also unpublished to date). Gross has computed tables of values of $E\mathcal{G}B^2W^3/P^2L^2$ for both three-point and four-point loading by using the procedure of boundary collocation of the Williams form of the Airy stress function mentioned earlier. The expressions for $E\mathcal{G}_{Ic}B^2W^3/P^2L^2$ as cubics in a/W, given in figures 30(b) and (c) (p. 56) for the three-point and the four-point loaded specimens, respectively, were obtained by applying least-squares best-fit procedures to these results of Gross. It is worthy of note that Gross's results are in satisfactory agreement with published results of experimental compliance calibrations by Irwin, et al. for three-point loading (ref. 15) and by Lubahn for four-point loading (ref. 32), as will be discussed in a forthcoming publication.

If the expressions for three-point and four-point loading given in figure 30 are compared, it will be apparent that, for a given a/W, the value of $E\mathcal{G}B^2W^3/P^2L^2$ is always less for three-point than for four-point loading, an average of about 10 percent less. This difference is consistent with the experimental results (refs. 15 and 32). The difference arises in the mathematical treatment because the computations for four-point loading considered the region within the minor span as subjected to a bending moment only, whereas the computations for three-point loading took into consideration the shearing stress that changes from $P/2BW$ to $-P/2BW$ at the center loading point.

The shearing stress is independent of L, whereas $\mathcal{G}$ is proportional to L^2/W^2, as mentioned previously. The influence of the shearing stress on $\mathcal{G}$ should therefore diminish with increasing L/W. For this reason, it is recommended that the span of a three-point-loaded specimen should not be less than $8W$, which is an unpublished estimate by Irwin. In the case of a four-point-loaded specimen the shearing stress is zero within the minor span, but it appears desirable that the major span should not be less than $8W$ in this case also. Furthermore, it is recommended that the minor span should not be less than $2W$ on the basis that the part of the strain energy field that is appreciably affected by the crack length is contained within the part of the specimen that extends a distance W on either side of the crack. Thus, with a minor span not less than $2W$, $\mathcal{G}$ should not be notably influenced by either the magnitude of the shearing stress outside the minor span or by the concentrated stresses at the loading points. From these considerations it is reasonable to expect that somewhat more accurate $\mathcal{G}_{Ic}$ measurements could be made with a bend specimen in four-point loading than with the same specimen in three-point loading.

In order to estimate the $\mathcal{G}_{Ic}$ measurement capacities of notched bend specimens the same criterion was used as in the case of the single-edge-notched tension specimen discussed previously. Values of $E\mathcal{G}/\sigma_{YS}^2W$ corresponding to $\sigma_{nom} = 3PL/B(W - a)^2 = \sigma_{YS}$ were calculated from the expressions given in figures 30(b) and (c) and used to plot the curves of EC_{Ig}/σ_{YS}^2W against a/W

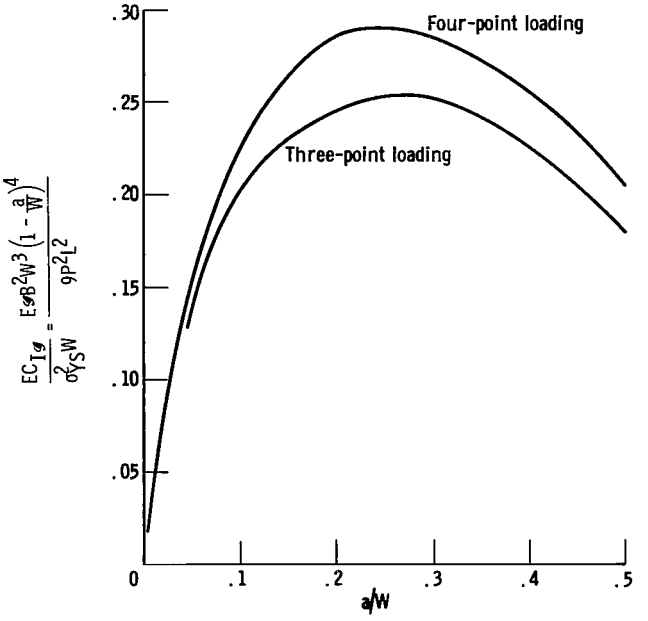

Figure 19. - Dependence of $EC_{I_g}/\sigma_{YS}^2 W$ on a/W for bend specimens.

shown in figure 19. From these two curves it is seen that the bend specimen is apparently used more efficiently in four-point loading than in three-point loading. This, of course, is simply a reflection of the fact that the values of $E\mathcal{G}B^2W^3/P^2L^2$ are greater for four-point than for three-point loading.

From comparison of figure 19 with figure 18, it is apparent that a single-edge-notched specimen loaded in four-point bending is about 15 percent more efficient than a single-edge-notched tension specimen of equal width and thickness and having D/W equal to 1/2. For a specimen loaded in three-point bending, however, the efficiency is about the same as that of the tension specimen. This, of course, involves the assumption that the same limiting condition applies to both types of specimens, which appears to be reasonable in the absence of experimental data to the contrary. It should be noted that, if the recommendations regarding specimen length, which are given in appendix A, are followed, the bend specimens would have to be about twice as long as the tension specimen of equal width.

Cracked Charpy Specimens

Considerable use has been made of cracked Charpy specimens for the intended purpose of $\mathcal{G}_{Ic}$ and even $\mathcal{G}_c$ measurements (ref. 33). The cracked Charpy specimen is simply a small, three-point-loaded bend specimen and is subject to exactly the same limitations as discussed for three-point bend specimens in general. The usual dimensions are as follows: W = 0.394 inch, B is variable between about 0.04 and 0.8 inch (for standard Charpy specimens, 0.394 in.), a_o is variable between about 0.1 and 0.2 inch (normally slightly greater than 0.1 in.), and the span is 1.574 inches. The specimen is produced by machining to normal Charpy-V dimensions, except that the thickness can be varied, and then by generating a fatigue crack at the bottom of the V-notch. It is tested either with a pendulum type impact testing machine, in which case it is usual to measure only the loss of pendulum energy, or in slow bending to obtain a load-deflection record.

It would be possible to determine $\mathcal{G}_{Ic}$ values, within the limitations of measurement capacity imposed by the dimensions of the Charpy specimen (C_{I_g} would be about $\sigma_{YS}^2/10E$), by measuring the pop-in load and proceeding as for any other three-point bend specimen. Although the ratio L/W is only about 2 for the Charpy specimen, rather than 4 as recommended for three-point-loaded

bend specimens, a $\mathcal{G}_{Ic}$ measurement that was accurate enough for some purposes, such as a materials screening program, might be obtained; however, this is not the way the specimen is usually treated. Instead, the loss of pendulum energy in an impact test, or the area under the load-deflection curve in a slow bend test, is measured. This energy value is usually denoted W, but here it will be called U in order to avoid confusion with the symbol for specimen width.

It is assumed that U can be equated with the energy required for the formation of new fracture surfaces only, and that no part of U is dissipated in any other way. Then a further assumption is made, essentially that the crack extension resistance is constant during the propagation of the crack through the specimen. With these assumptions it is concluded that $\mathcal{G}_c$, or $\mathcal{G}_{Ic}$ if the fracture is square, can be taken to be equal to U/A, where A is the area of the fractured cross section $B(W - a_o)$. Both of these assumptions are open to considerable question, and do not appear to have been thoroughly investigated. In fact, it can be inferred from recent work by Krafft that the second assumption is definitely not generally valid (ref. 34).

It is true that there is qualified evidence of correlation between U/A and results of some $\mathcal{G}_c$ tests to a degree that suggests U/A may be a useful measurement for screening purposes. This is more likely to be the case when the fractures are predominantly square and $\mathcal{G}_c$ approaches $\mathcal{G}_{Ic}$, than when the thickness is such that the fully developed fracture of a plate specimen would be predominantly slant. In any case, in the opinion of the authors the results of cracked Charpy tests should not be used for any other purpose than preliminary screening of materials, at least until such time as the interpretation of the results is much better understood than at present. It is particularly important that U/A values should not be used in an attempt to calculate critical crack dimensions for structures since this might be dangerously misleading.

Surface-Cracked Plate Specimens

Details of this type of specimen, sometimes called a part-through crack specimen, are shown in figure 30(d) of appendix A. This type was originally introduced in order to investigate directly the effects of cracks similar to those from which fractures had often originated in service (refs. 35 to 37). Cracks of controlled size, approximately semielliptical in shape with the major axis at the surface, were formed in plate specimens by fatigue stressing (refs. 37 and 38), or by static stressing in a suitable environment (ref. 36). It became possible to calculate $\mathcal{G}_{Ic}$ values from the results of tests of surface-cracked specimens when Irwin derived an appropriate expression for $\mathcal{G}_I$ (ref. 14, originally a private communication in 1960) by making use of earlier work by Green and Sneddon (ref. 39). Irwin's expression is given in figure 30(d) for the value of $\mathcal{G}_I$ in the central region of the front of a semielliptical surface crack that is no deeper than one-half the plate thickness. The expression as given includes a plastic zone correction term. The magnitude of $\mathcal{G}_I$ varies with position along the crack front and is greatest at the central position (ref. 14). The crack extends first in this region, and the magnitude of $\mathcal{G}_I$ at other positions along the crack front is of no consequence to this discussion.

Reference 14 does not deal with the question of how narrow the plate specimen could be without appreciably influencing the value of $\mathcal{G}_I$ at the middle of the crack front. It will be assumed rather arbitrarily, that W should not be less than 6c, where 2c is the surface length of the crack, assumed to be the major axis of an ellipse. This restriction is almost certainly on the safe side since the length of the pertinent central region of the crack front, where the crack first extends, is a small fraction of 2c.

Extended discussion of the $\mathcal{G}_{Ic}$ measurement capacity of surface-cracked specimens as a function of the various dimensions of the cracked section, W, B, a, and c (fig. 30(d)) would be unwarranted since the selection of this type of specimen would be governed by considerations other than measurement capacity. Instead the $\mathcal{G}_{Ic}$ measurement capacity will be estimated for a selected example in which the crack dimensions are as large as the aforementioned restrictions permit, namely, $a = B/2$ and $2c = W/3$. It is also assumed that $a/c = 1/2$, which is a likely ratio for specimens fatigue cracked in bending, and that the average net section stress at instability should not exceed σ_{YS} for a valid $\mathcal{G}_{Ic}$ test. Using these conditions in the expression for $\mathcal{G}_{Ic}$ given in figure 30(d) gives $C_{Ig} = 1.09\ \sigma_{YS}^2 B(1 - \nu^2)/E$, which is equal to $\sigma_{YS}^2 B/E$ when Poisson's ratio is 0.3. Here C_{Ig} is given in terms of B rather than in terms of W as for other types of plate specimens. The reason for this difference is that it is the depth of the crack that determines the $\mathcal{G}_{Ic}$ measurement capacity of a surface-cracked specimen, and the crack depth is limited to a maximum of one-half the specimen thickness.

In $\mathcal{G}_{Ic}$ tests with the surface-cracked type of specimen, it has been the usual practice to measure only the maximum load sustained in the test and the initial crack dimensions and to calculate $\mathcal{G}_{Ic}$ from these measurements. This practice assumes that instability occurs at maximum load and is not preceded by a metastable crack extension at some lower load. While the experience of the authors and examination of data obtained by others suggest this assumption is not seriously in error, at least as far as high-strength materials are concerned, it ought nevertheless to be subjected to critical investigation. It is recommended that crack extension should be monitored during all tests of surface-cracked specimens, just as for other types of specimens, by using one of the methods discussed under INSTRUMENTATION AND PROCEDURE. Results obtained without this sort of instrumentation should be regarded as somewhat uncertain, the more so the less brittle the material.

Circumferentially Notched Round Bars

Tensile testing of notched round bars has an extensive history, and it was natural that this type of specimen should have been one of the earliest used for $\mathcal{G}_{Ic}$ measurement. As in the case of notched bend specimens, it was not at first appreciated that notch sharpness equivalent to that obtained by fatigue cracking was necessary for accurate $\mathcal{G}_{Ic}$ measurement, so that much of the earlier $\mathcal{G}_{Ic}$ data is of somewhat doubtful value.

There is, at present, no highly accurate expression for $\mathcal{G}_I$ for a round

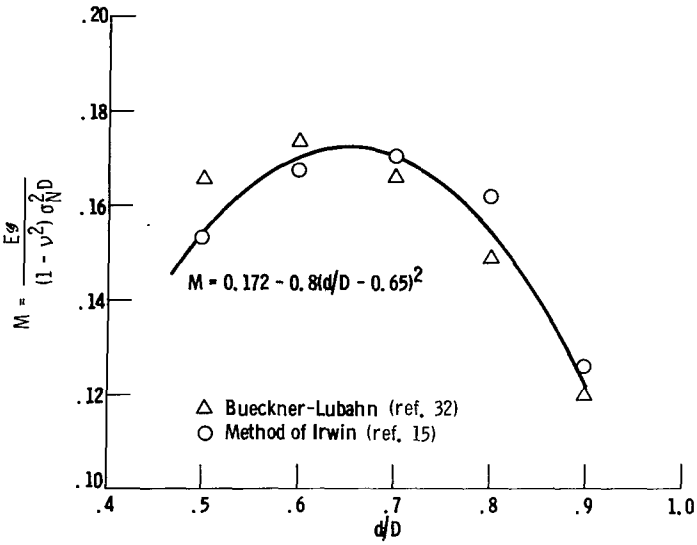

Figure 20. - Values of dimensionless factor M for round notched bars as function of d/D. $E\mathcal{G}_I = M\sigma_N^2 D(1 - \nu^2)$.

notched bar. An accurate solution would require an analysis of the type suggested by Sneddon (ref. 40). The mathematics involved in this type of approach is quite formidable. Approximate expressions for $\mathcal{G}_I$ are available from unpublished work by H. Bueckner of General Electric Co. Schenectady, New York (which is discussed by Lubahn (ref. 32) and Wundt (ref. 41)), or can be derived from stress concentration factors as discussed in reference 15. The results obtained by these approximate methods can be expressed conveniently in the form $E\mathcal{G}_I/(1 - \nu^2) = M\sigma_N^2 D$, where M is a dimensionless function of d/D, D is the major diameter, d is the diameter of the crack-notched section, and $\sigma_N = 4P/\pi d^2$ is the average net section stress.

Figure 20 shows values of the dimensionless factor M plotted against d/D. One set of plotted points is derived from results given in reference 32 and the other set was obtained by the method of reference 15. It is difficult to judge the accuracy of these values, but the extent of the agreement between them may give some indication. A fitted curve corresponding to a simple expression for M is also shown in the figure. Within the range of d/D shown, which is greater than would normally be of practical interest, the simple, compact expression for M appears to fit the plotted points adequately. Consequently, in the expression for $\mathcal{G}_{Ic}$ given in figure 30(e), the factor M has been replaced by $0.172 - 0.8(d/D - 0.65)^2$. Figure 20 also shows that the most efficient value of d/D is about 0.7, which corresponds to a notched cross-sectional area equal to about one-half the shank cross-sectional area. There would be no good reason for using a value of d/D much different from 0.7, so that the expression for $\mathcal{G}_{Ic}$ need only be used over a very limited range of d/D. In the range of d/D from 0.65 to 0.7, the assumption that M has the constant value 0.17 is probably all that is warranted by the accuracy of the available estimates.

The value of d that should be used in calculating a value of $\mathcal{G}_{Ic}$ is less than the measured value of the initial crack diameter d_o by a plastic zone correction term $E\mathcal{G}_{Ic}/3\pi\sigma_{YS}^2$. This is equivalent to increasing the initial crack depth $(D - d_o)/2$ by the same plane strain plastic zone correction term used for other types of specimens. It is worth mentioning that there is some arbitrariness about the choice of the value used for this term (ref. 29), which is apt to cause confusion in reading the literature unless one is aware of it. The practical effect, however, is negligible since it amounts to a small variation of a small correction term.

The ASTM Special Committee on Fracture Testing has recommended that the size of a round notched bar for $\mathcal{G}_{Ic}$ measurement should be sufficient to ensure that the average net section stress at fracture does not exceed 1.1 times the uniaxial tensile yield strength (ref. 9). The reason that the maximum recommended ratio of σ_N/σ_{YS} can be greater in this case than the ratio of σ_{net}/σ_{YS} for symmetrically cracked plate specimens is, of course, that the effective yield strength of the notched section of the round bar is correspondingly higher than σ_{YS}. A state of triaxial tension exists within the notched section and, on the basis of either a maximum shear stress or an octahedral shear stress criterion, the average net section stress at which yielding occurs will exceed σ_{YS} to an extent depending on d/D. For d/D equal to 0.7 or less the effective yield strength will be high enough to justify $\mathcal{G}_{Ic}$ measurements with values of σ_N at least up to 1.1 σ_{YS}.

Applying this limitation and taking the maximum value of M as 0.17 yield the estimated $\mathcal{G}_{Ic}$ measurement capacity of a notched round bar: $C_{Ig} = 0.22\ \sigma_{YS}^2 D(1 - \nu)/E$, or $0.2\ \sigma_{YS}^2 D/E$ when Poisson's ratio is 0.3. This calculation takes into account the plastic zone correction term. It is interesting to note that this estimate implies that the magnitude of C_{Ig} is just about the same for a notched round bar as for a symmetrically cracked plate specimen of width equal to the diameter of the notched round bar. The experimental results reported in reference 21 are consistent with this conclusion, and it is also intuitively apparent if one regards a symmetrically edge-cracked plate specimen as equivalent to a longitudinal slice from the center of a round notched bar.

The round notched bar requires a considerably greater amount of material and considerably more loading capacity than any of the other types of specimen for $\mathcal{G}_{Ic}$ measurement considered. To compensate for this, the potential accuracy of $\mathcal{G}_{Ic}$ measurement is probably relatively higher, but it would not be easy to attain the full potential accuracy. Apart from the need for a more accurate expression for $\mathcal{G}$ than is now available, it would be necessary to ensure almost perfect concentricity of fatigue cracking and uniformity of loading. No study has yet been made of the errors that would result from small deviations from the assumed perfectly uniform tensile loading of notched round bars, but the study of single-edge-notched plate specimens discussed earlier indicates that unavoidable nonuniformity of loading could be a considerable source of error in testing notched round bars. At the present time, the best accuracy of $\mathcal{G}_{Ic}$ measurement with notched round bars is probably no better than with plate specimens.

As in the case of surface-cracked specimens, it is usually assumed that instability occurs at maximum load in a notched round bar test, and $\mathcal{G}_{Ic}$ is calculated from the maximum load and the average diameter of the initial cracked section. In this case also the assumption ought to be subjected to adequate experimental verification utilizing crack extension monitoring instrumentation.

TABLE I. - COMPARISON OF DIMENSIONS OF VARIOUS PLANE STRAIN CRACK TOUGHNESS SPECIMENS HAVING C_{Ig} EQUAL TO σ_{YS}^2/E

[Specimens of the dimensions given would be large enough to measure values of $\mathcal{G}_{Ic}$ up to σ_{YS}^2/E, according to the criteria discussed in the text. For other values of $\mathcal{G}_{Ic}$ the minimum dimensions are directly proportional, and the loads are proportional to the square of the values given in the table.]

	Symmetrically cracked plate	Single edge notched			Surface cracked	Notched round
		Tension; D/W = 1/2	Bending; three point	Bending; four point		
Relative dimensions of initial cracks	$2a_o/W = 0.3$	$a_o/W = 0.3$	$a_o/W = 0.2$	$a_o/W = 0.2$	$a_o/B = 1/2$ $2c_o = W/3$	$d_o/D = 0.7$
Width or diameter of specimen, W or D, in.	5.0	4.0	4.0	3.5	6.0	5.0
Thickness of specimen, B, in.	0.65	0.65	0.65	0.65	1.0	---
Minimum length, in.	20	16	36	32	24	20
Load divided by yield strength, P/σ_{YS}, sq in.	1.8	0.8	0.14	0.16	5.4	11.2
Accuracy; order of merit	1	1	3	2	Potentially high	Potentially high

Summary Comparison of Specimens for $\mathcal{G}_{Ic}$ Measurement

In selecting a particular type of specimen for $\mathcal{G}_{Ic}$ measurement, the following factors may need to be considered: (1) the magnitude of the highest value of $E\mathcal{G}_{Ic}/\sigma_{YS}^2$ expected among the materials to be tested, (2) the desired accuracy of $\mathcal{G}_{Ic}$ measurement, (3) the loading capacity of available testing machines, (4) the economical usage of available test material, and (5) the form of the test material.

Table I provides guidance regarding necessary dimensions and load requirements, and suggests an order of merit of accuracy for the various types of specimen considered herein. The proportions given for each specimen type are considered to be about optimum so far as can be estimated at the present time. The dimensions given are estimated as the smallest that could be used for determination of a value of $\mathcal{G}_{Ic}$ equal to σ_{YS}^2/E, based on the criteria discussed in the preceding sections and subject to the qualifications stated therein. These values may need to be revised when sufficient pertinent experimental data have been accumulated, but it is unlikely that the revised values will be

appreciably smaller than those given in table I, more likely they will be greater. To estimate minimum dimensions for different values of $\mathcal{G}_{Ic}$, the linear specimen dimensions should be taken in direct proportion to the values given in table I, and the required load proportional to the square of the value given in the table. The safest course in deciding on the size of specimen to be used is to overestimate substantially the largest value of $E\mathcal{G}_{Ic}/\sigma_{YS}^2$ among the materials that are to be tested and to calculate the specimen dimensions accordingly. For most purposes, it is best to select from a graded series of specimen sizes, in which the linear dimensions increase by a factor of two from one size to the next. Following the ASTM Special Committee on Fracture Testing, one size of each type of plate specimen would be 3 inches wide. Hence, a graded series of plate specimens could conveniently have widths of three times 2^n inches, where n has the values -2, -1, 0, 1, 2, etc.

While it is somewhat premature to be very definitive about accuracy, experience so far suggests that the best accuracy of $\mathcal{G}_{Ic}$ measurement likely to be achieved is of the order of ±2 percent. A clear distinction should be made between testing accuracy and material variability. The variance of $\mathcal{G}_{Ic}$ for a given stock of material may be of the order of 10 percent or more; that is, the standard deviation of the results from a large number of accurate replicate tests would be of the order of 10 percent or more of the average value. It is important, however, to know the variability of the toughness of a material as well as its average toughness. In fact, a lower confidence limit is more important than the average value. For this reason it is desirable that the $\mathcal{G}_{Ic}$ measurement precision should be substantially better than the variance of $\mathcal{G}_{Ic}$ resulting from inherent material variability. The main factors that influence the accuracy of $\mathcal{G}_{Ic}$ measurement are the accuracy of the expression used for calculating $\mathcal{G}$ and the degree of uncertainty in the estimate of the effective crack length, including the plastic zone correction factor. The other necessary measurements can be made with relatively high accuracy (providing that the $\mathcal{G}_{Ic}$ instability is clearly defined). The authors believe that the accuracy of the expression for $\mathcal{G}$ for the single-edge-notched tension specimen (fig. 30(a)) is of the order of ±1/2 percent when $2a_o/W$ is about 0.3 (ref. 23). This is considerably better than the ±2 percent suggested for best attainable $\mathcal{G}_{Ic}$ measurement accuracy. The potentially more accurate expressions for $\mathcal{G}$ that might be obtained for the symmetrically cracked plate, the surface-cracked plate, and the notched round bar are therefore probably only of academic interest. The order of merit for accuracy given in table I is based on these considerations and on other points discussed in connection with bend specimens.

Reference to table I shows that if the loading capacity of available testing machines is the major limiting factor, a notched bend specimen will have a distinct advantage in the level of $E\mathcal{G}_{Ic}$ that can be measured with a given load. On the other hand, if material economy is of major importance because the amount of test material available is limited, then the single-edge-notched tension specimen requires only about half as much material as the bend specimen because it is proportionately shorter. It is also somewhat more accurate, but requires about five times as much load.

Both the surface cracked plate and the notched round bar types of specimens have a considerable disadvantage in the loading capacity required to mea-

sure a given level of $E\mathcal{G}_{Ic}$. Both also require considerably more material than the other types of specimen. It is possible, though not yet established, that either the surface-cracked plate specimen or the notched round bar might be useful for $\mathcal{G}_{Ic}$ measurement in cases where definitive results could not be obtained by the pop-in measurement procedure. In this case, of course, symmetrically cracked or single-edge-notched plate specimens of sufficient thickness could also be used, but then the advantage of lower bulk would largely be lost. This is a question that has yet to be settled by careful experiment. It is of considerable practical importance in connection with materials of high toughness and low yield strength that require large specimens.

Sometimes the controlling factor in selecting a specimen type will be the form of the stock of material to be tested and its texture in relation to the directions of the nominal principal stresses in service. For a given stock of material, $\mathcal{G}_{Ic}$ may depend considerably on the orientation of the crack in relation to the principal textural directions deriving from the ingot structure and subsequent deformation into product form. Alternatively, the measurement of toughness of welds and associated heat-affected regions may be of prime importance in a particular application. This requires very careful location of test cracks in relation to the variable structure of the weld region.

For the common case of plate stock, the nomenclature of reference 6 is convenient in referring to the six principal systems of crack propagation. The plate thickness direction is labeled T, the major rolling direction R, and the width direction W. The six principal systems of crack propagation can then be distinguished by pairs of letters, the first letter representing the normal to the crack plane and the second letter the direction of propagation. For example, RW would represent a crack normal to the rolling direction propagating in the width direction. It would be convenient to use either symmetrically cracked plate specimens or single-edge-notched specimens of full plate thickness for tests of either WR or RW, but surface-cracked plate specimens would be more convenient for WT or RT. Bend specimens could conveniently be used for any of these four systems of crack propagation. Tests of TW and TR present difficulties, but, fortunately, high tensile stresses in the thickness direction are usually avoided by good design. Sometimes heavy forgings may have to be used in such a way that the maximum nominal tensile stress is normal to the fibering direction, however, and in such cases it is most important to test appropriately oriented fracture toughness specimens. If necessary, extension pieces could be welded to test sections taken from the forging. In this case the obvious precautions should be observed.

INSTRUMENTATION AND PROCEDURE

From the foregoing sections, it is clear that the determination of $\mathcal{G}_c$ or $\mathcal{G}_{Ic}$ requires a knowledge of the crack length corresponding to the load at fracture instability. Essentially, two cases may be distinguished; namely, an appreciable amount of crack extension takes place before unstable fracture, or fracture instability occurs immediately from the initial crack front. The first case is frequently encountered in plane stress testing and the method of crack detection employed must be capable of following substantial amounts of

stable crack extension up to the maximum load. On the other hand, the major requirement in the second case is high sensitivity to initial crack movement as would be required in pop-in plane strain $\mathcal{G}_{Ic}$ testing. In special circumstances, however, it may be desirable to follow crack extension from pop-in to final fracture and in such cases the instrumentation must combine adequate sensitivity with the necessary measurement range.

Before proceeding with a description of the various types of instrumentation that have been employed for crack extension measurement, it is desirable to discuss the use of staining fluids for this purpose. In the first report of the ASTM Special Committee (ref. 5), it was suggested that a useful indication of crack length at fracture instability could be obtained by introducing a staining substance, such as India ink, into the notch or crack before starting the test. The assumption was made that the ink would follow only the stable crack extension. At fracture instability, the crack velocity would suddenly increase to a point where the ink would not longer move inward fast enough to keep pace with the crack tip. Even if this assumption could be proved correct, there are very good reasons for avoiding the use of staining agents. Thus, there is no way to determine, in advance, how much fluid must be introduced into the crack. An excess of fluid will splatter or run after fracture so that the crack length can be greatly overestimated. An insufficient amount of the staining agent will, of course, have the opposite effect. For these and other reasons, the Committee no longer recommends the use of staining fluids in crack toughness tests (ref. 9).

In the following section, several crack extension measurement methods potentially capable of yielding unambiguous results are described. Particular attention is given to practical applications and proper handling of the data. It should be emphasized that, with the exception of cinematography, all of the techniques have been developed recently, and only limited data are available. For these reasons some areas of uncertainty exist in the application of the new methods. It is also the purpose of this section to define these areas clearly.

CINEMATOGRAPHY

Synchronized motion-picture cameras may be used to photograph simultaneously the load dial of a tensile machine and the plane surface of a specimen containing a through-the-thickness crack. Satisfactory resolution of the crack requires adjustment of the lighting for the particular surface conditions of the specimen being tested. Unwanted reflections can be minimized by use of polarizing screens (ref. 9). The film is examined frame by frame and the crack length directly measured. Some investigators have made this measurement to include the apparent extent of the dimple ahead of the crack with the idea of taking into account directly a plastic zone correction; however, this procedure cannot be generally recommended since the apparent extent of the dimple will vary with the prevailing lighting conditions.

The data are generally represented as a plot of crack length and applied load (or gross area stress) against time (or frame number). Examples of such plots are shown in figure 21 for wide sheets of 4330M steel provided with cen-

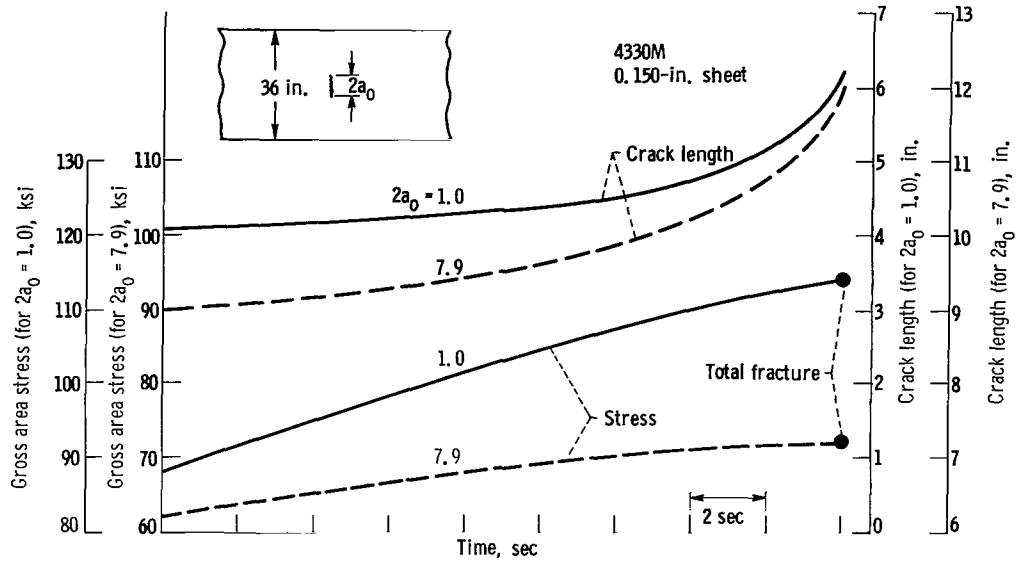

Figure 21. - Examples of stress and crack length measurements using cinematography.

ter fatigue cracks (unpublished data obtained by C. F. Tiffany, Boeing Aircraft Co.). From representations of this type, the crack length at maximum gross stress may be selected for use in calculating the fracture toughness; however, some investigators select the stress at a crack length judged to correspond to the onset of "fast crack acceleration." Obviously, such a criterion for selection of crack length permits considerable latitude in the judgment when behaviors such as those shown in figure 21 are encountered. For this reason, it is recommended that the stress and crack length at maximum load be used in the fracture toughness calculations, in accordance with the recommendations of the ASTM Special Committee on Fracture Testing (ref. 5).

This photographic method has been widely employed by the aircraft industry in tests on very wide thin-sheet specimens containing long through-the-thickness slots or cracks. The materials of interest in these tests are quite tough and generally exhibit considerable stable crack extension. Under these circumstances, the technique has considerable flexibility in that it may be readily adapted to tests at both low and high temperatures providing the specimen surface is visible. The method is unsuitable for pop-in detection since it provides no indication of crack extension below the surface. As presently used, it is relatively insensitive to small crack extensions, however, there is no fundamental reason why considerable increase in sensitivity could not be obtained by suitable refinements in the optical system.

ELECTRICAL POTENTIAL MEASUREMENT

If a body carrying a current contains a discontinuity, there will be a disturbance of the potential field in the region of the discontinuity. If the discontinuity is a crack, the potential difference between two fixed points spanning the crack will increase as the crack extends providing the total cur-

rent does not decrease. This is the basis for crack extension measurement by the electric potential method. In practice, a constant current is supplied to the specimen, and potential probes are fastened at suitable points on either side of the crack. The potential change with crack length may be measured with a double Kelvin bridge as used by Steigerwald and Hanna (ref. 42), or by electronic instruments such as the milliohmmeter employed by Anctil, Kula, and DiCesare (ref. 43) or a highly sensitive voltmeter-amplifier described later. These electronic instruments have the advantage that an output is provided suitable to drive an X-Y plotter.

The potential distribution will be a function of the specimen geometry, crack size, and location of the current leads. As shown previously (ref. 43), it is possible to obtain a calibration curve that relates E/E_o to the crack size, where E is the potential difference between the probe points measured as a function of load and E_o is the value at no load for a specimen without a crack. A calibration curve of this type will be independent of the material and specimen size provided that all dimensions are changed in proportion including the locations of the current and potential leads. For specimens containing through-the-thickness cracks, it is convenient to make a pattern of the specimen geometry by using electrically conductive analog paper. These paper patterns are useful not only in obtaining the calibration curve, but also for general potential mapping of a particular specimen geometry in order to determine optimum locations for the current leads and potential probes. A sufficiently constant current can be maintained if the paper is connected across a 90-volt dry battery through a resistor having a value about 100 times the resistance of the paper pattern. A razor blade may then be used to cut the desired crack lengths and shapes, and a vacuum tube voltmeter employed to map the potential field. The recommended current input and probe locations as well as the calibration curves to be described were obtained in this manner.

Testing Procedure

The specimen should be electrically insulated from the tensile machine by some suitable means, such as polytetrafluoroethylene sheet spacers or electrical insulating tape. It is desirable to locate the current leads sufficiently far from the crack plane so that small variations in their position would not influence the results. This distance should be greater than one-half the width or diameter of the practical specimen types illustrated in appendix A. For high sensitivity to initial crack extension, the potential probes should be located as close to the crack tip as possible, the actual location depending on the method of attachment. The probe positions shown in figure 22 for plate specimens were established for use with a particular set of slotted yokes that span the specimen thickness and reference the specimen edges. Opposing pointed screws in each yoke serve as probes contacting the front and rear surface of the specimen. Leads from each yoke connect to the potential measuring device. It will be noted that the yokes locate the probes slightly behind the nominal initial position of the crack tip of the practical plate specimens shown in appendix A. This horizontal location is chosen so that the tip of the shortest crack (within the expected tolerance) will be at or beyond the probe points.

The constant current may be obtained from a regulated power supply. These

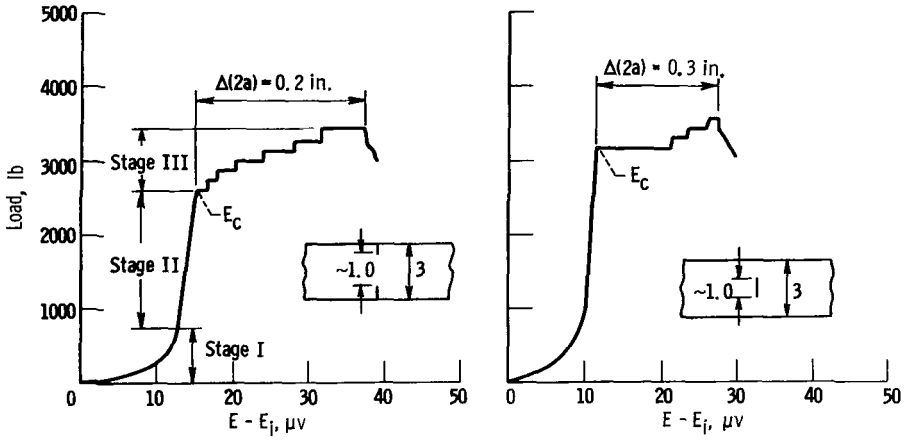

Figure 22. - Typical load as function of potential records illustrating pop-in and crack extension to maximum load.

are commercially available in capacities up to 100 amperes with high stability. Alternatively, wet storage cells connected in parallel can be used with a suitable ballast resistance (high relative to the specimen) in series with the specimen. If the current output drifts appreciably during a test, additional batteries should be connected in parallel to reduce the current drain per cell. The current supply cable can be connected to the specimen by clamps or by bolts through small holes. With the latter arrangement, the holes should be at least one specimen width or diameter away from the crack to avoid interaction of stress fields. The amount of current required for a given crack extension sensitivity will, of course, depend on the resistivity of the specimen, its cross section, and the sensitivity of the potential measuring device employed. As an example, the authors, using the potential sensing and recording equipment described in the following section, obtained the desired sensitivity to crack extension when supplying 10 amperes to a steel single-edge-notched specimen 3 inches wide and 1/2 inch thick.

As mentioned previously, an electronic potential measuring instrument can be used to advantage. The milliohmmeter described by Anctil, et al. (ref. 43) has a built-in power supply that is limited to 100 milliamperes. This instrument therefore lacks sufficient sensitivity to make it generally useful in fracture testing. A recently developed (ref. 44) voltmeter-amplifier combination can be used with an external current supply, such as those just described, and has an output of 10 volts for full-scale meter deflection on any one of 13 input ranges, the most sensitive of which is 0 to 0.1 microvolt. Zero suppression is available up to 100 times full scale on any range. In order to minimize the influence of thermal emf's, it is necessary to avoid, where possible, dissimilar metal junctions in the input circuit to the voltmeter. Difficulties due to these thermocouple effects and stray fields limit the useful working range of the voltmeter to 30 microvolts or higher unless elaborate precautions are taken in the experimental setup.

Reduction of Data

If the output of the voltmeter-amplifier is fed to one channel of an X-Y

recorder and the signal from a load cell to the other channel, a plot of potential against load is obtained directly. Examples of two such plots for single-edge-notched specimens are shown in figure 22 illustrating both a relatively small initial crack movement and a very distinct pop-in.

The initial potential E_i is suppressed and the potential change with load $E - E_i$ may be considered as consisting of three stages. During stage I there is a rapid increase in potential at low loads due to separation of the fatigue crack surfaces. The potential during stage II increases linearly with load and corresponds only to elastic strain. The beginning of stage III, E_c, is marked by a nonlinear increase in potential resulting from crack extension and/or crack tip plasticity (the contribution of plasticity is usually considered negligible). The accuracy with which the load corresponding to initial crack movement can be established depends on the sharpness of the division between stage II and stage III. In the two cases shown this is quite distinct; however, as will be discussed later (see fig. 28, p. 53), small amounts of crack extension may occur early in the test before a distinct pop-in, and, in such cases, acoustic measurements are of assistance in interpretation of the potential records. If plane strain toughness determinations are to be made, the load at pop-in is read directly from the load-potential records and used in the appropriate $\mathcal{G}_I$ equation. Also the load-potential records may be converted to a plot of crack extension as a function of load by the use of calibration curves.

Calibration curves for several practical fracture toughness plate specimen types are given in figures 23 and 24. These curves have been determined for the potential probe positions shown and with the current input attachments far enough removed that the measured potential is influenced only by the crack. When these curves are used, the value of E_o could be measured on a dummy specimen without a notch. Alternatively, E_o for a particular test may be calculated as follows

$$E_o = \frac{E_c + E_i}{A}$$

where A is the value of E/E_o obtained from the calibration curve corresponding to the measured initial crack length and width and E_c is the potential at crack initiation (see fig. 22).

When calibration curves of this type are used, it is important to keep in mind certain restrictions on their application. For the probe positions and connections described, the calibration curves for symmetrically cracked plate specimens will yield the average of the crack extension occurring at each crack tip. Independent measurements are of course possible, if separate pairs of probes are used at these locations. The calibration curve corresponds to a crack front normal to the specimen surface and load axis. As discussed previously (see fig. 6, p. 9) in an actual specimen, the front is always curved, and this curvature in mixed mode fractures may occupy a region about equal to the plate thickness. For this reason, crack extensions calculated from the calibration curves will closely approximate the actual values only when the curved region is a small fraction of the total crack extension. In $\mathcal{G}_c$ tests, the effect of curvature on measured crack length may be neglected if the total crack length $2a_m$ is large in comparison with the thickness.

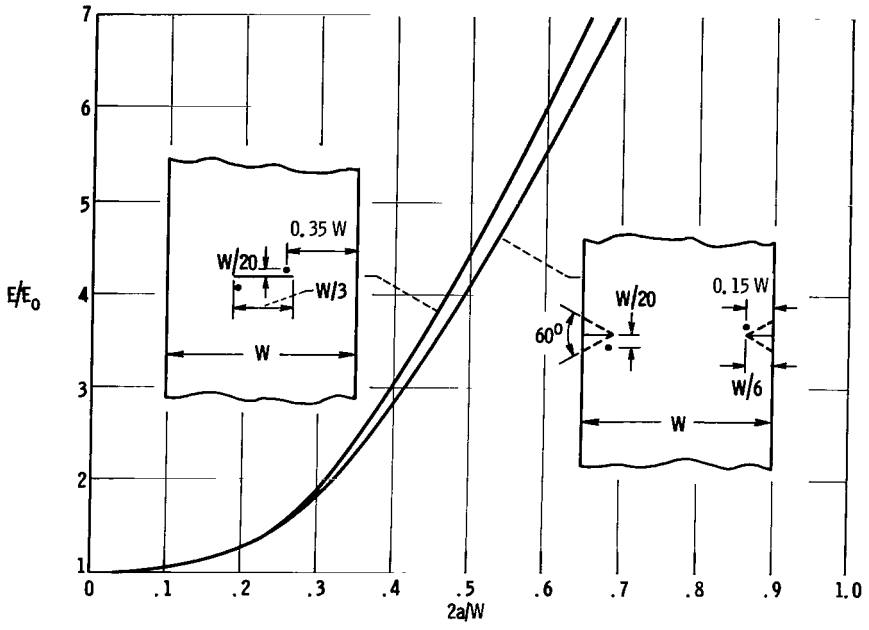

Figure 23. - Electric potential calibration curves for symmetrically center- and edge-cracked plate specimens.

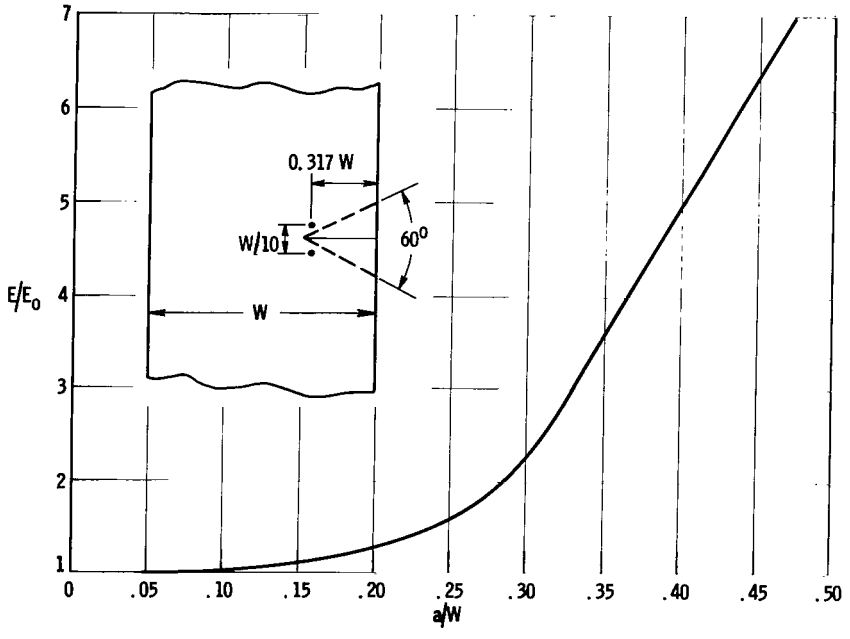

Figure 24. - Electrical potential calibration curve for single-edge-notch specimen.

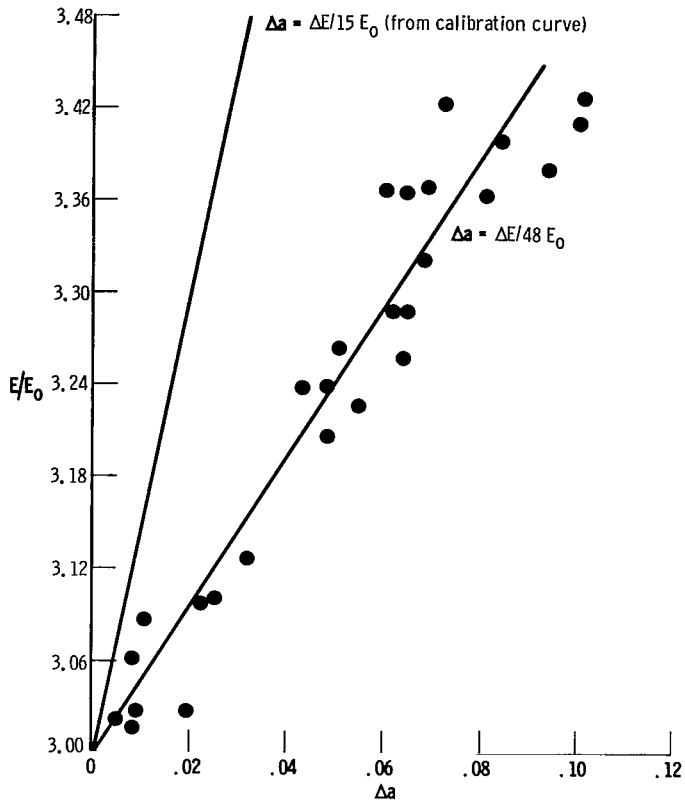

Figure 25. - Ratio of potential change to initial potential as function of actual crack extension determined by interrupted tests.

When studies are made of the pop-in phenomenon, it is instructive to determine the extent of crack movement associated with a given indication of pop-in (e.g., the magnitude of a step in the loading curve). As discussed previously, the calibration curves are not particularly useful in this case since the major portion of the crack extension is occupied by the curved fracture front. To obtain a more direct indication of crack extension under these circumstances, interrupted tests of a series of specimens may be made representing increasing amounts of potential change. The specimens are heat-tinted to outline the crack front and then broken. A plot may then be made of E/E_o at interruption against some measured value from the heat-tinted crack indication.

A few results of this type have been reported in reference 42. Some data obtained by the authors is shown in figure 25 for single-edge-notch tests on 18Ni-Co-Mo steel aged to a wide range of strength levels. In this case Δa represents the maximum extension from its initial position of the most advanced point on the crack front. Within the scatter, there is roughly a linear relation between Δa and E/E_o that is useful in estimating the amount of crack extension represented by a given potential change at pop-in. The general trend of these points may be compared with the slope of the calibration curve for the particular value of a_o/W used in these tests. As might be expected, the calibration curve would give estimates of Δa corresponding to a straight crack front and therefore considerably smaller than the actual values.

Advantages and Limitations of Potential Method

This technique appears to be readily adaptable to all practical fracture toughness specimen types. The necessary instrumentation is commercially available to permit automatic recording of the potential change. Calibration curves relating potential change to crack extension may be easily determined for through-cracked specimens by use of analog paper. With optimum location of the potential probes, a very high sensitivity to crack extension may be obtained. For example, it may be reasonably assumed that 0.050 inch chart pen movement on the X-Y recorder is easily discernible and that a gain of 100,000 is possible

through the voltmeter-amplifier with good stability. This corresponds to a sensitivity of 0.5 microvolt. With this sensitivity, a crack extension of 0.0025 inch is obtained from the calibration curve for an aluminum center-cracked specimen (W = 3 in. and B = 1/2 in.) provided with 50 amperes.

The current requirements can constitute a definite limitation on the use of the method. Thus, the resistivity of most metals decreases very rapidly at temperatures below about -300° F, and at liquid-hydrogen temperature, the current required for normal specimen sizes would be prohibitively large. At elevated temperatures, the resistivity increases but appreciable thermoelectric effects become difficult to avoid. The speed of testing is limited by the response of the potential measuring device employed. When the high-sensitivity electronic voltmeter described previously is used, the maximum response speed is of the order of 1/2 second. The use of an oscilloscope is apparently not possible because input amplifiers are not available that have sufficient gain combined with fast response, high stability, and low noise.

DISPLACEMENT GAGES

The displacement per unit load between two points spanning a crack will increase with crack length. For elastic loading, this ratio is defined as a compliance and, for given specimen dimensions, depends only on the distance between the points (gage length) and the elastic modulus of the material. Measurement of displacement is the basis for use of so-called compliance gages in measuring the crack extension in fracture toughness specimens. In practice a test specimen is provided with a gage that measures the displacement as a function of applied load as the crack extends. It is usually assumed that the compliance corresponding to any point on the curve may be obtained from the slope of a line connecting this point to the origin.

The crack length at a given load is then determined with the aid of a calibration curve. For example, in the case of symmetrically loaded plate specimens, this curve gives the ratio of $2a/W$ as a function of C/C_o, where C is the assumed compliance corresponding to a particular point on the load extension curve, and C_o is the compliance at zero crack length. The value of C_o may be calculated from the elastic modulus, as is described later. The calibration curve in this form will apply to any material, providing that all dimensions of the specimen under test and the gage length are proportioned to the calibration specimen. Calibration curves are obtained by machining progressively longer slots (simulating the crack) into a calibration specimen and determining the compliance for the selected gage length at each known slot size for conditions of elastic loading.

This method of determining crack extension is well suited to tensile-loaded plate specimens containing through-the-thickness cracks although, in principle, it applies to any specimen. Application to other specimen types, however, offers as yet unresolved problems either in the experimental procedure or in the interpretation of the results. For example, the method has been applied to circumferentially notched round bars as described in reference 32 and more recently by Van der Sluys (ref. 45). The data obtained indicate that the change in compliance with crack extension is relatively small for this specimen

type and that eccentricities of loading (which are difficult to avoid) can have an appreciable effect on the accuracy.

Before proceeding to a discussion of the practical application of displacement gage techniques for crack extension measurement, it should be mentioned that the strain energy release rates can be determined from the rate of change of compliance with crack length. This technique for determining $\mathcal{G}$ values for a particular specimen geometry was suggested in reference 31 and was used in reference 32 to obtain an experimental relation between strain energy release rate and crack depth in bend specimens and circumferentially notched round bars. A more recent publication (ref. 23) describes a very precise method for measuring the compliance of tensile-loaded plate specimens as a function of crack length and gives results for a single-edge-notched specimen.

Gage Types and Testing Procedures

The requirements for a displacement gage to be used in $\mathcal{G}_c$ tests are somewhat more difficult to meet than those for $\mathcal{G}_{Ic}$ testing. For the former application, it would be desirable to use a single calibration curve for a given specimen type. This requires that the gage length be adjustable to accommodate various specimen sizes. This, in turn, requires the signal output as a function of displacement to be linear over a sufficiently wide range to accommodate the largest displacements anticipated. On the other hand, the main requirement of the displacement gage in $\mathcal{G}_{Ic}$ testing is that of high sensitivity to initial crack movement. For either type of testing the gage length should be as short as possible as an aid in obtaining maximum sensitivity.

Linear response to displacement combined with high sensitivity and adequate range for $\mathcal{G}_c$ testing is provided by linear differential transformers. A recent paper by Boyle (ref. 46) describes a fixed gage length (2 in.) adapter that permits the use of a standard releasable extensometer for displacement measurements between gage points spanning the center notch in plate specimens. A magnification factor of 2 is provided by a lever system with spring-loaded knife edges. The adapter is not completely separable, and the gage points suffer rather badly when testing hard specimens to fracture. It is difficult to construct a trouble-free displacement gage with a variable gage length. A design of this type for center-notched specimens used by Jones and Brown (ref. 47) consists of an upper and lower split yoke. These are attached independently to the specimen so that the gage is completely separable. One yoke contains the differential transformer and the other serves as a reference surface for the transformer core. The yokes are provided with gage points that span the notch at the specimen center. A particular gage length is established by use of a positioning jig that is removed after clamping the yokes to the specimen. This gage is adaptable to any specimen thickness and, in principle, could be made to accommodate a range of specimen widths. In order to permit its use on specimens having an appreciable bow, an additional linear differential transformer should be incorporated so that the strains on the two flat surfaces of the specimen may be averaged. In an arrangement used by Bulloch and Ferguson (ref. 48) a linear differential transformer and a suitable reference surface are fastened to the specimen by means of pins fitted through small holes. This method of direct attachment appears to be limited to situations where the

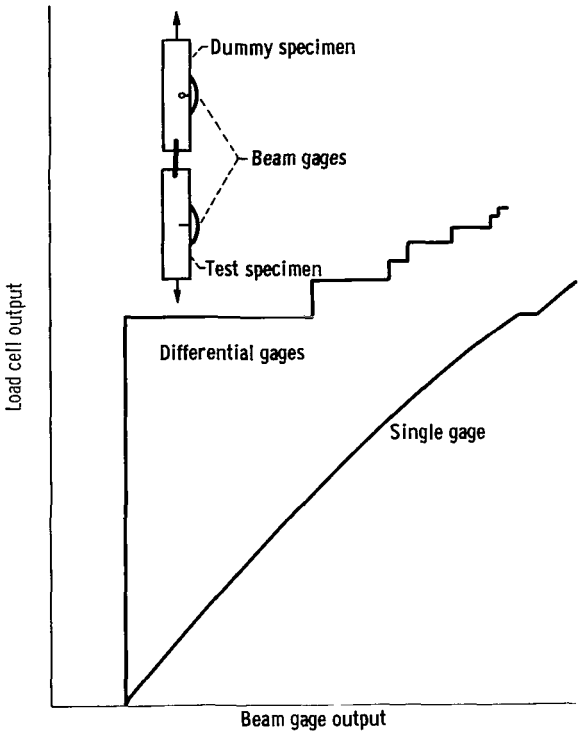

Figure 26. - Load-displacement records for single-edge-notch specimen obtained by using single beam gage and differential beam gage.

specimen thickness is sufficient to support the pins; however, it does have the advantage of flexibility.

It is possible to drive the load-strain recorder of some tensile machines directly from a linear differential transformer output; however, when some types of transformer are used in the displacement gage, additional circuits may be required to obtain the desired magnification factor. If the transformer output is to be fed to an X-Y recorder, it is necessary to employ a suitable converter.

As indicated previously, requirements regarding the measuring range and linearity of output may be relaxed in $\mathcal{G}_{Ic}$ testing. Relaxation of these requirements gives more freedom in the design of displacement gages that are frequently optimized for a particular specimen type. The linear differential transformer gages described previously are, in general, also suitable for $\mathcal{G}_{Ic}$ testing. In the case of single-edge-notched specimens, a standard releasable or separable extensometer may be clamped at the specimen edge across the notch; however, an extensometer used in this way can be damaged if the specimen halves are allowed to rotate freely about the loading pins after fracture. Excessive rotation can be prevented by placing soft metal blocks in the yokes under the specimen ends. For bend tests, Romine (ref. 49) has described the use of a conventional deflectometer to measure deflections at the point of load application.

Frequently, it is possible to use a relatively simple beam gage (or clip gage) that consists of a metal strip with wire resistance or foil strain gages on opposite faces. The beam gage is then bent to bear against two reference surfaces at the extremes of the gage length. Sensitivity of a beam gage increases with the ratio of beam thickness to length and the ratio of gage length to beam length. A description of highly sensitive gages of this type is given in reference 23. Beam gages are readily adaptable to a variety of testing situations. For example, the gage may be located by edge grooves machined on either side of the notch in single-edge-notched specimens. The output of a beam gage will be a nonlinear function of its end deflection; however, this is of no particular consequence in $\mathcal{G}_{Ic}$ testing, where a pop-in indication is the only information required.

A differential beam gage is under development by the authors to detect pop-in in single-edge notched specimens. The principle is to buck out that part of the gage output that is not due to a change in crack length. The arrangement is shown schematically in figure 26. The test specimen is loaded

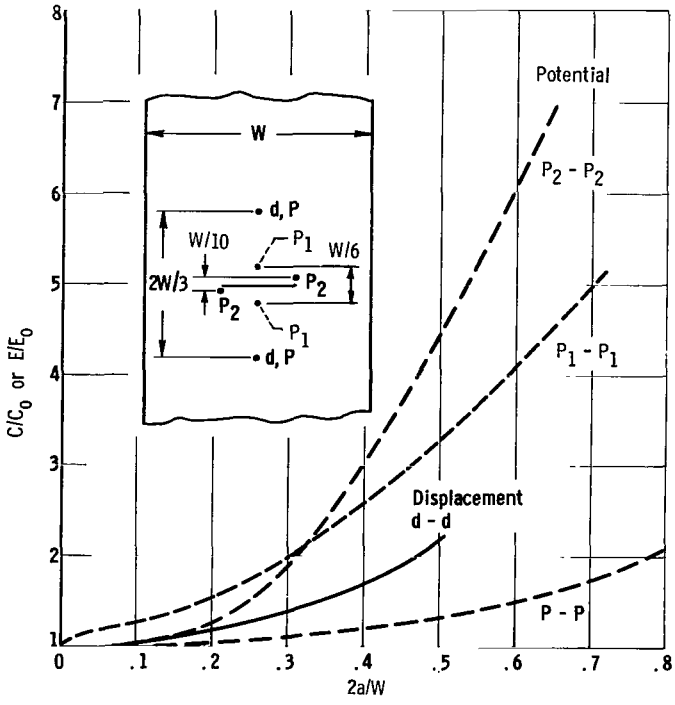

Figure 27. - Comparison of displacement-gage calibration curve with several calibration curves obtained by using electric potential measurements illustrating influence of gage length.

in tandem with a dummy specimen. Both specimens are provided with beam gages spanning the edge cracks, the output of these gages being opposed in a suitable bridge arrangement. The dummy specimen is identical to the test specimen except that its edge slot is terminated in a hole rather than in a fatigue crack, so that no crack extension in the dummy occurs during the test. A schematic X-Y recorder plot of gage output against applied load, shown in figure 26 for a single-edge-notched specimen, illustrates results obtained with a differential beam gage and a single gage. Two advantages of the differential beam gage compared with a single gage are evident. Because the differential gage output is obtained only with crack extension, pop-in indications will be more distinct and considerably higher gain may be used without exceeding the limits of the chart paper before pop-in occurs.

The instrumentation necessary for beam gages is the same as that normally employed with wire resistance strain gages. The gage outputs can be used to drive conventional tensile machine load-strain recorders either directly or through commercially available adapters. If an X-Y recorder is used, the gage bridge output may be connected directly to one axis with the output from a load cell bridge on the other.

Reduction of Data

If plane strain toughness determinations are to be made, the load at pop-in is determined from records such as those shown in figure 26 and used with the appropriate $\mathcal{G}_{Ic}$ equation (see appendix A). If the load-strain record has been determined with gages designed for $\mathcal{G}_c$ testing, the deflections may be converted to crack lengths by using a suitable calibration curve. A calibration curve given in reference 46 for center-notched specimens is shown in figure 27, along with some curves for the same specimen geometry obtained by the previously discussed potential method. The displacement gage calibration is given as C/C_o against $2a/W$, where C is the compliance corresponding to any point on the load-displacement curve and C_o is the compliance for zero crack length. This calibration curve applies to all center-notched specimens providing that the displacement gage used has a gage length of $2W/3$ and is

located symmetric to the crack plane at the specimen centerline. Under these conditions, $C = e/P$, where e is the total measured deflection at the load P. The value of C_o for this gage length may be calculated as follows

$$C_o = \frac{2}{3EB}$$

where B is the thickness and E is the elastic modulus of the test specimen.

This procedure for use of the calibration curve assumes that the unloading line corresponding to any given amount of crack extension on a load-displacement curve will be linear and will pass through the origin. Actually, as shown in reference 46, the unloading curves are not exactly linear and do not pass through the origin. This is attributed to the action of a crack tip plastic zone that acts to prop open the crack on unloading. By adjusting the unloading curve to pass through the origin, it is assumed that this propping effect is subtracted out and that the "true" compliance at load is determined.

It should be noted that the displacement measurements will be increased by crack tip plasticity as well as by crack extension. For this reason, it has been suggested that the crack lengths calculated from the displacement-gage calibration curves be used directly in the $\mathcal{G}_c$ equations since, in effect, they already contain a plasticity correction. While this procedure should probably be followed, it is difficult to establish it on a firm basis due to the previously discussed complexities introduced by the nonideal unloading curve behavior.

When interpreting displacement-gage data in terms of crack extensions, it should be remembered that, at best, only average values can be determined unless the crack extension is large in comparison with the thickness. Measurement errors associated with small crack extensions due to the curved nature of the crack front were previously discussed in connection with data reduction from potential measurements.

Advantages and Limitations of Displacement Gages

This method, in principle, is adaptable to a wide variety of testing situations, but the particular gage design will depend on both the specimen type and the testing conditions. If linear differential transformers are employed, the gage may be immersed directly in a cryogenic bath. The authors have used differential transformers at liquid-hydrogen temperatures with no difficulty, providing that the transformer windings were sealed against moisture. By employing conventional extensometer extension arm arrangements, linear differential transformer displacement gages could be used for high-temperature tests.

A beam-displacement gage for $\mathcal{G}_c$ testing at high temperatures with center-notched plates was described by Morrison, Jenkins, and Kattus (ref. 50). The gage is mounted between extension arms that contact the edges of the specimen near the heads and extend out the sides of a split infrared lamp furnace. Because of the fact that the gage points are far removed from the crack, this

gage has rather low sensitivity. Beam gages with foil-resistance sensing elements could be used at cryogenic temperatures. A discussion of the most suitable types of foil gages for use in liquid hydrogen, and special precautions regarding their application have been presented by Kaufman (refs. 51 and 52).

The beam displacement gage is particularly well suited to $\mathcal{G}_{Ic}$ testing at high strain rates because the output may be easily displayed on conventional oscilloscopes. The authors have used these gages on single-edge-notched specimens fractured in the order of a few milliseconds. Care must be taken to design the gage and arrange the mounting so that the rapid application of load does not cause resonance vibration in the beam.

There appears to be no inherent limitation to the application of displacement gages in fracture toughness testing. As compared with the electrical potential technique, however, the method of adapting the sensing element to the specimen is frequently more difficult. This is particularly true of the linear gages desirable for $\mathcal{G}_c$ testing, which may require carefully machined and sometimes complex mounting and linkage systems. Another disadvantage lies in the fact that unwanted bending deflections will cause nonlinear response and require the use of double sensing elements to cancel the bending effects.

Sensitivity of Displacement Gages

It has been generally assumed that this crack measurement method is inferior to the electrical potential technique regarding the sensitivity available. This observation is probably based on the rather large apparent difference in slopes between the calibration curves that have been published for these two methods. In order to define more clearly such differences, a calibration curve for the center-notched-plate displacement gage described in reference 46 is compared (fig. 27) with calibration curves obtained for the same specimen type by using potential measurements. From this representation it is quite evident that the slope of the calibration curves depends on the gage length and position selected. In this respect, the potential measurement has an advantage since the probes can be located very close to the crack tips; however, it should be noted that, for identical locations and gage lengths, Boyle's displacement-gage calibration curve has a definitely greater slope than that obtained by electric potential measurements. From this displacement-gage calibration curve, an estimate was made regarding the absolute sensitivity to crack extension that could be obtained in a typical case.

The case selected as an example is represented by a load-deflection curve given in reference 46 for a 3/16-inch-thick by 3-inch-wide 7075-T6 center-notched specimen. With the assumption that a chart pen deflection of 0.050 inch is easily discernible and a magnification of 2000, a total crack extension of 0.006 inch should be detectable at the pop-in load, which was about 16,000 pounds. This may be compared with the 0.003-inch crack extension sensitivity previously mentioned for the electrical potential method when used on an aluminum single-edge-notched specimen and assuming the same minimum pen deflection for a pop-in indication. These calculated sensitivities, of course, are not directly comparable in a quantitative sense and should not be taken as limiting

values. They do indicate, however, that both the displacement gage and potential method can have very high sensitivity to crack extension.

ACOUSTIC METHOD

Disturbances within a material that result in the sudden release of elastic energy can frequently be detected by using a transducer that will convert an elastic vibration into an electrical signal. Thus, if a piezoelectric crystal is placed in contact with a specimen containing a propagating crack, the crystal will produce signals that may be amplified and recorded or used to drive a loud-speaker. The acoustic method of detecting crack propagation has been described by Romine (ref. 53) and Jones and Brown (ref. 47). Reference 47 contains a detailed description of the method including the electronics required for recording load and crack sounds.

In practical application, a crystal transducer such as a slightly modified phonograph pickup is clamped to the specimen or to the loading train. A tape recording is made of the load and specimen acoustic output simultaneously on separate channels. The tape record may then be transferred to a recording oscillograph or simply audited with the tape load channel working a counter. The method is extremely sensitive to small crack extensions and may give definite indications of crack movement before either an electrical potential or a displacement gage gives a discernible output. While the amplitudes of the acoustic signals probably increase with the amount of material involved in a given increment of crack movement, there is no known way of estimating the amount of crack extension from acoustic records. For this reason, the acoustic technique is best used in conjunction with either potential measurements or displacement gages. Employed in this way, it provides additional information concerning the initial stage of the crack propagation process.

Examples of Data

As shown in reference 47, the acoustic method is capable of indicating pop-in loads that agree well with those obtained by using displacement gages. In some cases, the acoustic method may also be helpful as an aid in interpreting a load-potential or displacement record. In order to illustrate this point, two examples are shown in figure 28 for single-edge-notch tests on an 18Ni-Co-Mo steel aged at 725° and 800° F. In this representation, load-potential records are given along with corresponding indications from oscillograph traces of the acoustic output. These tests were interrupted at the point indicated, heat tinted to outline the fracture area, and then pulled to failure. Two rather different behaviors are represented by these tests.

The specimen aged at 800° F exhibited an abrupt large potential change at about 10,000 pounds, and this corresponds to a large burst of sound. Preceding this burst, there were very weak acoustic indications possibly due to crack movement in fatigue-damaged metal. Approximately 0.1-inch total crack extension was represented by this pop-in, and the plastic zone size at pop-in was less than one-tenth the thickness. Under these circumstances, there seems to

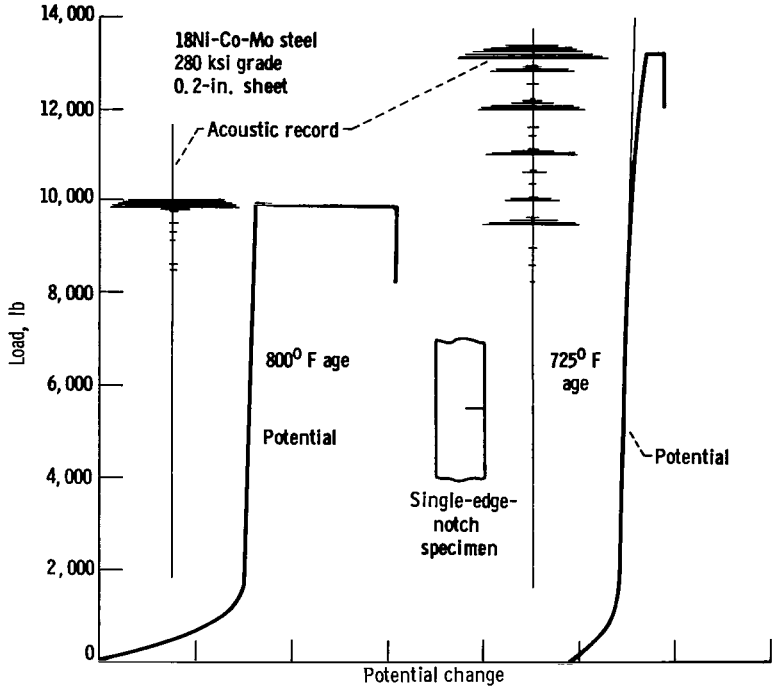

Figure 28. - Load-potential and acoustic records from single-edge-notch specimens illustrating different pop-in behaviors.

be little doubt that the load at fracture instability in the opening mode has been measured.

The behavior of the specimen aged at 725° F appears more complex. There is a distinct step in the load-potential curve at about 13,400 pounds, and this corresponded to about 0.025-inch total crack extension. The plastic zone size at this pop-in was approximately one-eighth the specimen thickness. It will be noted that rather strong acoustic indications start at about 9500 pounds and continue with increasing load. Using the acoustic indications as a guide makes it possible to detect a slight departure from linearity in the potential record also starting at about 9500 pounds. Apparently, a substantial portion of the 0.025-inch total crack extension at pop-in took place at considerably lower loads. There is a question as to whether the pop-in load observed for the specimen aged at 725° F can be used to calculate a K_{Ic} having the same meaning as that calculated from the pop-in obtained from the specimen aged at 800° F.

Advantages and Limitations of Acoustic Method

The major advantage of the acoustic method lies in its relative simplicity and adaptability to a variety of specimen types and testing situations. For example, if the specimen is enclosed in a furnace or low-temperature bath, the pickup may be mounted on some part of the loading train external to the specimen enclosure. Special precautions must be taken, however, to eliminate the introduction of extraneous sounds that might mask or be confused with crack movement indications. As a general rule, it is desirable to establish independently the background noise character and level before conducting a series of tests. Frequently, this may be accomplished by loading a smooth specimen under the same conditions as to be used for the notch tests. As mentioned previously, a major disadvantage of the acoustic method is the fact that there is as yet no way of quantitatively relating the signal characteristics to the extent of crack movement.

CONTINUITY GAGE

A recent paper by Kemp (ref. 54) describes the use of a "continuity" gage to measure crack extension. Essentially, this is a special type of foil-resistance strain gage and is constructed in the same general way. It consists of regularly spaced metal ribbon elements all connected in parallel and is applied to the specimen surface so that the elements are normal to the direction of crack propagation. The elements are longer the farther they are from the notch tip. This arrangement provides approximately linear resistance change as successive elements are fractured by the extending crack.

In its present form, each gage is about 1/2-inch wide and has 20 elements with a spacing of approximately 0.01 inch. If crack extensions beyond 0.2 inch are expected, additional gages are placed in the line of crack extension. Conventional strain gage instrumentation may be used with each gage being part of a bridge circuit. The output of the bridge is recorded on a light-beam galvanometer oscillograph along with a load trace from a load-cell bridge circuit. A step appears in the output for each ribbon element fractured, and the crack length at maximum load can be determined by counting these steps.

The main advantage to this type of gage is its adaptability to crack growth studies in tank tests at cryogenic temperatures. The gages are rather expensive and, of course, are not reuseable.

Lewis Research Center,
National Aeronautics and Space Administration,
Cleveland, Ohio, October 16, 1964.

APPENDIX A

PRACTICAL FRACTURE TOUGHNESS SPECIMENS - DETAILS OF PREPARATION, TESTING, AND DATA REPORTING

The various practical fracture toughness test specimens are shown in figures 29 and 30. The proportions given are those developed in previous sections of this report. Relations for $\mathcal{G}$ and K are given in the usual closed form for symmetrically cracked tension specimens (figs. 29(a) and (b)), and for the surface-cracked plate specimen (fig. 30(d)). Polynomial expressions in a/W are shown in figure 30 for the single-edge-notched plate and bend specimens. The sources of these expressions are discussed in the text. It will be noted that the factor $1 - \nu^2$ has been used in the equations relating $\mathcal{G}$ to K for plane strain. This factor is an approximation in relation to the stress state in an actual plate specimen. This point is discussed further in the section PRACTICAL SPECIMEN TYPES: Plastic Zone Connection Term - $\mathcal{G}_{Ic}$ and K_{Ic} Calculations. As mentioned in the text, it is difficult to judge the accuracy of the published approximate solutions for $\mathcal{G}_I$ for circumferentially notched round bars. The form shown in figure 30(e) represents an average of several results in the d/D range between 0.55 and 0.9.

SPECIMEN MACHINING

The most critical features of specimen machining are concerned with the preparation and location of the fatigue crack starter notches and the means for

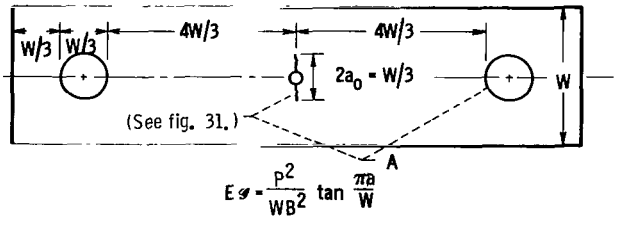

(a) Symmetrical center-cracked plate.

For $\mathcal{G}_c$ tests	For $\mathcal{G}_{Ic}$ tests
$16 < W/B < 45$	$5 < W/B < 10$
$E\mathcal{G} = E\mathcal{G}_c = K_c^2$	$E\mathcal{G} = E\mathcal{G}_{Ic} = (1 - \nu^2)K_{Ic}^2$
$a = a_m + \frac{E\mathcal{G}_c}{2\pi\sigma_{YS}^2}$	$a = a_m + \frac{E\mathcal{G}_{Ic}}{6\pi\sigma_{YS}^2}$

A - Surfaces must be symmetric to specimen centerline within W/1000

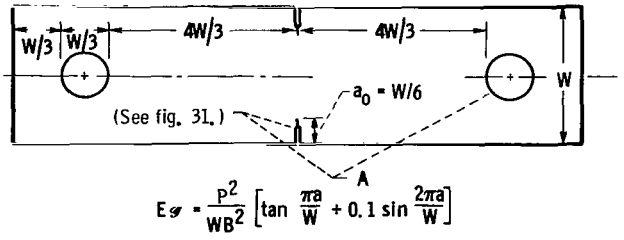

(b) Symmetrical edge-cracked plate.

Figure 29. - Practical fracture toughness specimen types. Specimens for general use. (The factor $1 - \nu^2$ is an approximation. See appendix.)

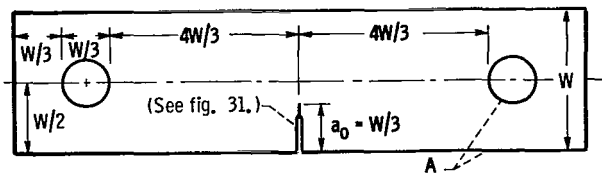

(a) Single-edge-notched plate (tension).

$4 < W/B < 8$

$$E\mathcal{G}_{Ic} = \left(\frac{P}{B}\right)^2 \frac{1}{W}\left[7.59\frac{a}{W} - 32\left(\frac{a}{W}\right)^2 + 117\left(\frac{a}{W}\right)^3\right]$$

$$E\mathcal{G}_{Ic} = (1-\nu^2)\,K_{Ic}^2$$

A - Surfaces must be true to specimen centerline within W/1000

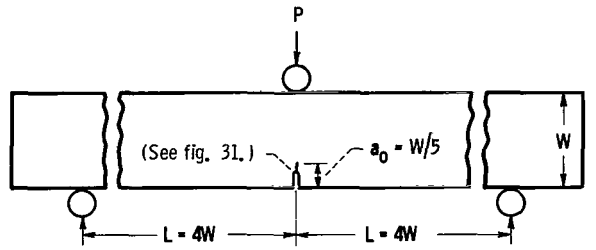

(b) Notch bend specimen (three-point loaded).

$2 < W/B < 8$

$$E\mathcal{G}_{Ic} = \left(\frac{P}{B}\right)^2 \frac{L^2}{W^3}\left[31.7\frac{a}{W} - 64.8\left(\frac{a}{W}\right)^2 + 211\left(\frac{a}{W}\right)^3\right]$$

$$E\mathcal{G}_{Ic} = (1-\nu^2)\,K_{Ic}^2$$

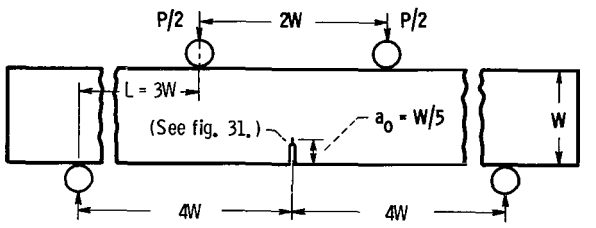

(c) Notch bend specimen (four-point loaded).

$2 < W/B < 8$

$$E\mathcal{G}_{Ic} = \left(\frac{P}{B}\right)^2 \frac{L^2}{W^3}\left[34.7\frac{a}{W} - 55.2\left(\frac{a}{W}\right)^2 + 196\left(\frac{a}{W}\right)^3\right]$$

$$E\mathcal{G}_{Ic} = (1-\nu^2)\,K_{Ic}^2$$

Figure 30. - Practical fracture toughness specimen types. Plane strain tests. (For all specimens, $a = a_0 + E\mathcal{G}/16\pi\sigma_{YS}^2$; the factor $1-\nu^2$ is an approximation. See appendix.)

transmitting the load to the specimen. Details of the starter notches for plate tension specimens are shown in figure 31. The dimensional limits given will ensure that the influence of the shape of the notch does not extend to the tip of the fatigue crack. The angle at the slot end is not critical and the notch tip radius shown may be easily produced by slightly extending the 1/16-inch slot with a 0.010-inch jewelers saw. If the starter notches shown in figure 31 cannot be accommodated because of insufficient specimen width, it is best to produce narrow slots by using an electric-discharge machining process. An indentation made with a sharp chisel having a rounded end will serve as a crack starter for the surface-cracked specimens. Alternatively, a surface notch may be produced by an electric-discharge process. The V-notch in the circumferentially notched round bar should have as sharp a tip radius as possible in order to minimize the stress necessary to produce fatigue cracks in a reasonable length of time.

Where loading pin holes are shown, these should serve as reference surfaces for machining the crack starter notches. In this way, symmetry of the notches about the loading axis is easiest to achieve. It should be noted that the pin hole position in relation to the width is an important parameter in the single-edge-notched plate specimen and that the $\mathcal{G}_I$ expression shown applies to the W/2 position with the limits indicated. No means for gripping the

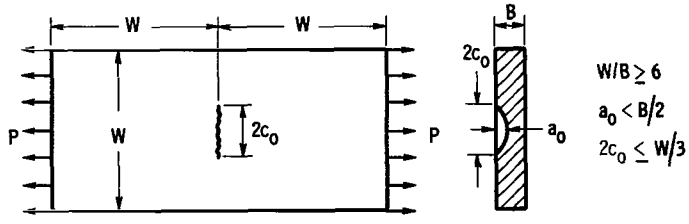

$$\frac{E\mathscr{G}_{Ic}}{1-\nu^2} = K_{Ic}^2 = \frac{1.2\,\pi P^2 a_0}{W^2 B^2}\left[\frac{1}{\Phi^2 - 0.2\left(\frac{P^2}{W^2B^2\sigma_{YS}^2}\right)}\right]$$

$$\Phi = \int_0^{\pi/2} \sqrt{1 - \frac{c_0^2 - a_0^2}{c_0^2}\sin^2\theta}\; d\theta$$

(d) Surface-cracked plate.

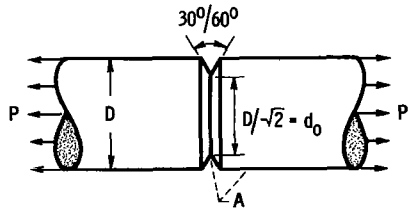

A - Surfaces must be concentric to within D/1000

$$\frac{E\mathscr{G}_{Ic}}{1-\nu^2} = K_{Ic}^2 = \frac{1.63\,P^2 D}{d^4}\left[0.172 - 0.8\,(d/D - 0.65)^2\right]$$

$$d = d_0 - \left(\frac{E\mathscr{G}_{Ic}}{3\pi\sigma_{YS}^2}\right)$$

(e) Circumferentially notched and fatigue-cracked round bar.

Figure 30. - Concluded. Practical fracture toughness specimen types. Plane strain tests. (For all specimens, $a = a_0 + E\mathscr{G}/6\pi\sigma_{YS}^2$; the factor $1 - \nu^2$ is an approximation. See appendix.)

surface-cracked plate specimen or the circumferentially notched round bar are shown in figure 30. Pin loading of the surface cracked specimen will require a head wider than the test section, or the use of doubler plates around the pin holes. Alternatively, the specimen may be gripped in the tensile machine jaws. The circumferentially notched round bar is normally provided with buttonheads, although as described in reference 8, a threaded specimen with special alinement surfaces may be used. In either case, precision machining of all cylindrical surfaces is necessary to ensure that the notch section is perpendicular to and concentric with the loading axis.

The edges of the plate tension specimens do not have to be machine-finished unless they serve as locating surfaces for positioning of the notches and pin holes. The flat surfaces of these specimens are machined only when necessary to remove warping or to eliminate an unwanted surface layer. Rectangular cross section bend specimens (figs. 30(b) and (c)) should provide no special machining problems whatsoever. Surfaces in contact with the loading

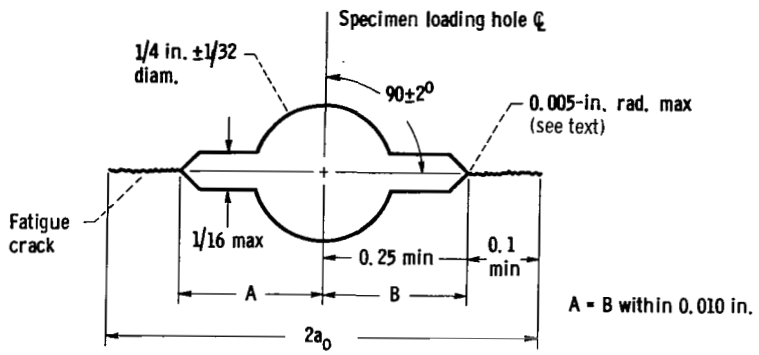

(a) Fatigue crack starter for center-cracked plate specimens (W ≥ 2 in.).

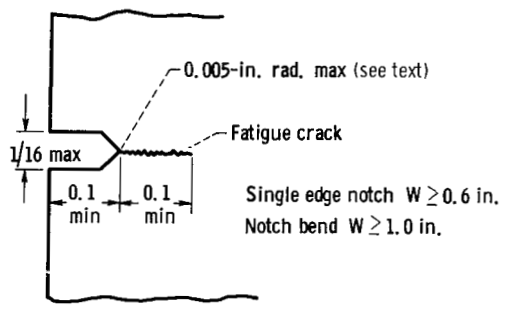

(b) Fatigue crack starter for edge-notched plate specimens.

Figure 31. - Fatigue crack starter notches for center-cracked and edge-notched plate specimens.

and support pins should be ground to reduce friction. These surfaces can then serve for reference purposes when machining the fatigue crack starter notch.

FATIGUE CRACKING AND HEAT TREATMENT

Details concerning the fatigue cracking of the symmetrically cracked tension specimens (figs. 29(a) and (b)) and the circumferentially notched round bar (fig. 30(e)) have been given in references 5 and 8. It was recommended that tension-tension loading be used to produce fatigue cracks in the symmetrically center cracked specimens; however, some investigators have cracked this type of specimen in bending with the moments perpendicular to the sheet plane. This method produces "wing cracks" starting from the surface and joining at the center of the thickness. These cracks are sometimes difficult to keep in one plane and form a crack front with considerable curvature. Further studies of these crack shapes are required before this method of producing fatigue cracks can be recommended.

Surface fatigue cracks may be produced by cantilever bending of the specimen over a support that tapers to a point. Details of this technique are given in references 37 and 38. Cracks are initiated more easily and may be located at the desired spot on the specimen surface if a small sharp indentation is provided as a crack starter. As mentioned previously, this starter notch may be produced by a chisel or by electric-discharge machining. The surface cracks produced by this method are semielliptical in shape with the ellipticity usually increasing with the depth; however, it is possible to control the crack shape, if the starter notch is produced by electric-discharge machining, by using specially contoured electrodes.

Fatigue cracking of single-edge-notched plate specimens may be conveniently accomplished by cantilever bending with the bending moment in the plane of the specimen. The stress at the notch tip is kept in tension with the minimum stress set just sufficient to ensure smooth operation of the fatigue machine and satisfactory alinement during the fatigue cycling. This method poses no special problems, and the cracks are relatively easy to control since they are running into a decreasing stress field.

There are very few data regarding the effect of the maximum stress used in producing fatigue cracks on the measured fracture toughness. Some results given in reference 39 for surface cracked specimens of a brittle steel indicate no significant difference in average K_{Ic} values for nominal bending stresses of about 30, 40, and 60 percent of the yield strength. The scatter of data, however, appeared to be greater as the nominal bending stress increased. In view of these results, it would seem best to keep the nominal net section stress below 50 percent of the yield strength when fatigue cracking.

The question of whether heat treating should precede or follow fatigue cracking is difficult to resolve with the limited amount of data now available. The center crack strength of a relatively brittle steel (ref. 5) was the same whether sheet specimens were heat treated before or after fatigue cracking. The results of a few surface crack tests (ref. 37) appear to confirm this behavior. It would seem reasonable to assume that any differences in fracture toughness due to the cracking - heat-treating sequence would tend to be minimized by stable crack extension. For this reason, the effects of this sequence should be more pronounced in $\mathcal{G}_{Ic}$ than in $\mathcal{G}_{c}$ tests. In this respect, recent experiments in the authors laboratory showed that more distinct pop-in indications were obtained for 18Ni-Co-Mo single-edge-notch tests when specimens were aged after fatigue cracking rather than before. In the absence of more definite information, it would seem reasonable to heat treat after fatigue cracking where possible. This procedure should assist in reducing any effects that might arise from differences in the fatigue stressing conditions; however, as pointed out in reference 8, when preparing circumferentially notched round bars, it may be necessary to finish machine and fatigue crack after full heat treatment in order to correct for warpage and to avoid quench cracks. These considerations may also be important for thick plate specimens.

TESTING PROCEDURE

Testing procedures for symmetrically cracked sheet tension specimens and circumferentially notched round bars have been discussed in references 5 and 8. As described in these publications, special care should be taken to minimize eccentricity of loading by using pin-yoke assemblies for sheet specimens and by using special loading devices for notched round bars. Details concerning a concentric buttonhead loading fixture for notched rounds are given by Jones and Brown (ref. 55). When testing thick pin-loaded specimens in tension, it is advisable to make use of double pin yokes in order to minimize bending moments acting both perpendicular and parallel to the sheet plane. These yokes must be carefully machined so that they do not in themselves introduce bending due to misalinement of the pin holes. When pin yokes are used, it is desirable to lubricate the pin holes with molybdenum disulfide.

As mentioned previously, surface-cracked specimens, if pin loaded, will require a head larger than the test section or the use of doubler plates around the pin holes. By using the tensile machine jaws for gripping, a uniform width and thickness specimen may be employed. It might be expected that loading in the jaws of a tensile machine would introduce considerable eccentricity, which would vary from test to test and produce excessive scatter; however, data from

a large number of replicate tests on jaw-loaded surface-cracked specimens of a brittle steel have been reported in reference 38 and exhibit very small scatter. In addition, a few results (ref. 37) for pin-loaded specimens indicate that surface cracks eccentric with respect to the specimen centerline do not result in lower strengths. On the basis of the data available, it would appear that jaw loading for this type of specimen is permissible; however, the data should be examined for scatter that could be attributed to variation in eccentricity from test to test.

In the case of heat-treated martensitic steels, crack extension can occur due to stress corrosion under a constant load in the presence of water vapor. Plane strain fracture toughness values for such materials can be influenced by the amount of water vapor in the air, and this effect will depend on the testing speed. Results are given in reference 45 for circumferentially notched round bars of SAE 4340 (σ_{YS} = 225,000 psi) tested at three levels of relative humidity using normal loading rates. Because of the limited amount of data available from this investigation and the scatter encountered, no quantitative relation could be established between the amount of moisture present and the fracture toughness; however, the notch strength decreased with increasing relative humidity. In view of the uncertainties involved, it is not possible to make any recommendations at this time concerning control of the humidity during a test; however, when testing low-alloy-tempered martensites or other alloys subject to stress corrosion in the presence of water, the temperature and relative humidity of the air surrounding the specimen should be recorded.

DATA REPORTING

The usefulness of fracture toughness data depends not only on the selection of proper testing techniques, but also on the proper identification of the reported data. All too frequently fracture toughness information appearing in the published literature and in company reports is so poorly identified that no judgment can be made concerning its validity nor its applicability to the particular problem at hand. It must be remembered that fracture testing and fracture mechanics analysis are new approaches to a very complicated problem and that in the formative stages of any engineering science it is necessary to provide the maximum amount of information to the person attempting to use the data. With this in mind, the Fifth Report of the ASTM Special Committee on Fracture Testing (ref. 9) listed required supplementary information that should be reported with fracture toughness data.

Care should be exercised to avoid using the designation "fracture toughness" or the symbols $\mathcal{G}$ or K in connection with data that do not meet the basic requirements for fracture toughness testing. A particularly dangerous practice is the reporting of calculated critical flaw sizes as a function of applied stress when the calculations are based on poorly established fracture toughness data. Information of this type should always be carefully qualified regarding the basis of calculation and the manner in which the fracture toughness parameters were obtained.

APPENDIX B

SYMBOLS

A	net cross-sectional area of cracked Charpy specimen
a	length, half-length, or depth of crack according to type of specimen, figs. 27 and 28
a_m	measured value of a at instability
a_o	initial value of a
B	thickness of plate or bend specimen
C	compliance of selected gage length of specimen, i.e., reversible change in gage length per unit load
C_o	initial value of C for specimen without crack
C_g, C_{Ig}	$\mathcal{G}_c$ or $\mathcal{G}_{Ic}$ measurement capacity of specimen, i.e., estimated maximum value of $\mathcal{G}_c$ or $\mathcal{G}_{Ic}$ that could be measured with acceptable accuracy for specimen of given dimensions made of material of given yield strength and elastic modulus
c	half-length of surface crack, fig. 30(d)
D	major diameter of round notched bar, fig. 30(e); distance of axis of loading from cracked edge of single-edge-notched tension specimen, fig. 17
d_o	average diameter of crack-notched section of round notched bar, fig. 30(e)
E	Young's modulus; electrical potential difference between two selected positions on specimen
E_o	value of electrical potential difference
e	displacement, i.e., change in selected gage length of specimen
$\mathcal{G}$	strain energy release rate with crack extension per unit length of crack border, or, crack extension force (crack extension mode unspecified)
$\mathcal{G}_I$	$\mathcal{G}$ for opening mode of crack extension
$\mathcal{G}_c, \mathcal{G}_{Ic}$	critical value of $\mathcal{G}$ or $\mathcal{G}_I$ at point of instability of crack extension, taken to be measure of fracture toughness of material

K	stress intensity factor of elastic stress field in vicinity of crack front (crack extension mode unspecified)
K_I	opening mode of crack extension
K_c, K_{Ic}	critical value of K or K_I at point of instability of crack extension, taken to be an alternative measure of crack toughness of material
L	effective length of fracture toughness specimen; moment arm length of bend specimen, i.e., half of difference between major and minor spans
M	dimensionless coefficient in expression for $\mathcal{G}$ for round notched bar
P	load applied to specimen
R	crack extension resistance of material at crack tip that opposes $\mathcal{G}$
r_Y, r_{IY}	plastic zone correction term added to measured crack length; subscript I applies to plane strain conditions and r_{IY} is taken to be $r_Y/3$
U	loss of pendulum energy in impact test, or, area under load-deflection curve of test of cracked Charpy specimen
W	width of plate specimen or depth of rectangular section beam specimen
ν	Poisson's ratio
σ	gross stress applied to specimen in tension, i.e., applied load divided by WB for plate specimen, or $\pi D^2/4$ for notched round bar
σ_c	σ at point of instability of crack extension
σ_N	net section stress for round notched bar
σ_{net}	average net section stress for a symmetrical plate specimen in tension
σ_{nom}	nominal stress at position of crack tip for a single-edge-notched tension specimen or bend specimen
σ_{YS}	uniaxial tensile yield strength (0.2 percent offset)

REFERENCES

1. Tipper, C. F.: The Brittle Fracture of Metals at Atmospheric and Sub-Zero Temperatures. Metallurgical Rev., vol. 2, no. 7, 1957, pp. 195-261.

2. Tipper, C. F.: Testing for Brittleness in Structural Steels. Brittle Fracture in Steel, Rep. P3, Admiralty Advisory Comm. on Structural Steel, Her Majesty's Stationery Office, 1962, pp. 132-150.

3. Pellini, W. S., and Puzak, P. P.: Fracture Analysis Diagram Procedures for the Fracture-Safe Engineering Design of Steel Structures. Report 5920, Naval Res. Lab., Mar. 1963.

4. Pellini, W. S., and Srawley, J. E.: Procedures for the Evaluation of Fracture Toughness of Pressure Vessel Materials. Rep. 5609, Naval Res. Lab., June 1961.

5. ASTM Special Committee on Fracture Testing of High-Strength Metallic Materials: Fracture Testing of High-Strength Sheet Materials. ASTM Bull. 243. Jan. 1960, pp. 29-40; ASTM Bull. 243, Feb. 1960, pp. 18-28.

6. ASTM Special Committee on Fracture Testing of High-Strength Metallic Materials: The Slow Growth and Rapid Propagation of Cracks. Materials Res. & Standards, vol. 1, no. 5, May 1961, pp. 389-393.

7. ASTM Special Committee on Fracture Testing of High-Strength Metallic Materials: Fracture Testing of High-Strength Sheet Materials. Materials Res. & Standards, vol. 1, no. 11, Nov. 1961, pp. 877-885.

8. ASTM Special Committee on Fracture Testing of High-Strength Metallic Materials: Screening Tests for High-Strength Alloys Using Sharply Notched Cylindrical Specimens. Materials Res. & Standards, vol. 2, no. 3, Mar. 1962, pp. 196-203.

9. ASTM Special Committee on Fracture Testing of High-Strength Metallic Materials: Progress in Measuring Fracture Toughness and Using Fracture Mechanics. Materials Res. & Standards, vol. 4, no. 3, Mar. 1964, pp. 107-119.

10. Irwin, G. R.: Fracturing and Fracture Mechanics. Rep. 202, Dept. Theoretical and Appl. Mech., Univ. Ill., Oct. 1961.

11. Irwin, G. R.: Fracture Testing of High-Strength Sheet Materials Under Conditions Appropriate for Stress Analysis. Rep. 5486, Naval Res. Lab., July 27, 1960.

12. Krafft, J. M., Sullivan, A. M., and Boyle, R. W.: Effect of Dimensions on Fast Fracture Instability of Notched Sheets. Proc. of Crack Propagation Symposium, vol. I, College of Aero. Cranfield (England), Sept. 1961, pp. 8-28.

13. Srawley, J. E., and Beachem, C. D.: Crack Propagation Tests of High-Strength Sheet Materials. Pt. IV - The Effect of Warm Pre-Straining. Rep. 5460, Naval Res. Lab., Apr. 1960.

14. Irwin, G. R.: Crack-Extension Force for a Part-Through Crack In a Plate. Jour. Appl. Mech. (Trans. ASME), ser. E, vol. 29, no. 4, Dec. 1962, pp. 651-654.

15. Irwin, G. R., Kies, J. A., and Smith, H. L.: Fracture Strengths Relative to Onset and Arrest of Crack Propagation. Proc. ASTM, vol. 58, 1958, pp. 640-660.

16. Bluhm, J. I.: A Model for the Effect of Thickness on Fracture Toughness, Proc. ASTM, vol. 61, 1961, pp. 1324-1331.

17. Irwin, G. R.: Fracture. Vol. VI of Encyclopedia of Phys., S. Flugge, ed., Springer (Berlin), 1958, pp. 551-590.

18. Irwin, G. R.: Fracture Mechanics. Structural Mechanics, Pergamon Press, 1960, pp. 557-594.

19. Irwin, G. R., and Srawley, J. E.: Progress in the Development of Crack Toughness Fracture Tests. Materialpruefung, vol. 4, no. 1, Jan. 1962, pp. 1-11.

20. Srawley, J. E., and Beachem, C. D.: Resistance to Crack Propagation of High-Strength Sheet Materials for Rocket Motor Casings. Rep. 5771, Naval Res. Lab., May 31, 1962.

21. Boyle, R. W., Sullivan, A. M., and Krafft, J. M.: Determination of Plane Strain Fracture Toughness with Sharply Notched Sheets. Welding Jour. (Res. Supplement), vol. 41, no. 9, Sept. 1962, pp. 428s-432s. (See also ASME Paper 62-MET-13, 1962.)

22. Gross, Bernard, Srawley, John E., and Brown, William F., Jr.: Stress-Intensity Factors for a Single-Edge-Notch Tension Specimen by Boundary Collocation of a Stress Function. NASA TN D-2395, 1964.

23. Srawley, John E., Jones, Melvin H., and Gross, Bernard: Experimental Determination of the Dependence of Crack Extension Force on Crack Length for a Single-Edge-Notch Tension Specimen. NASA TN D-2396, 1964.

24. Winne, D. H., and Wundt, B. M.: Application of the Griffith-Irwin Theory of Crack Propagation to the Bursting Behaviour of Disks, Including Analytical and Experimental Studies. Trans. ASME, vol. 80, 1958, pp. 1643-1655.

25. Ripling, E. J., Mostovoy, S., and Patrick, R. L.: Measuring Fracture Toughness of Adhesive Joints. Materials Res. & Standards, vol. 4, no. 3, Mar. 1964, pp. 129-134.

26. Westergaard, H. M.: Bearing Pressures and Cracks. Jour. Appl. Mech., vol. 6, no. 2, 1939, pp. A-29 - A-53.

27. Kies, J. A.: Aircraft Glazing Materials - A Method for Evaluating the Shatter Resistance of Aircraft Canopy Materials. Memo. Rep. 237, Naval Res. Lab., Nov. 1953.

28. Greenspan, Martin: Axial Rigidity of Perforated Structural Members. Jour. Res. Nat. Bur. Standards, vol. 31, no. 6, Dec. 1943, pp. 305-322.

29. Irwin, G. R.: Plastic Zone Near a Crack and Fracture Toughness. Proc. Seventh Sagamore Ord. Materials Conf. Syracuse Univ. Res. Inst., Aug. 1960.

30. Sullivan, A. M.: New Specimen Design for Plane-Strain Fracture Toughness Tests. Materials Res. & Standards, vol. 4, no. 1, Jan. 1964, pp. 20-24.

31. Irwin, G. R., and Kies, J. A.: Critical Energy Rate Analysis of Fracture Strength. Welding Jour. (Res. Supplement), vol. 33, 1954, pp. 193s-198s.

32. Lubahn, J. D.: Experimental Determination of Energy Release Rates for Notch Bending and Notch Tension. Proc. ASTM, vol. 59, 1959, pp. 885-915.

33. Orner, G. M., and Hartbower, C. E.: Sheet Fracture Toughness Evaluated by Charpy Impact and Slow Bend. Welding Jour. (Res. Supplement), vol. 40, Sept. 1961, pp. 405s-416s.

34. Krafft, J. M.: Fracture Toughness of Metals. Rep. of NRL Prog., Naval Res. Lab., Nov. 1963, pp. 4-16.

35. Beachem, C. D., and Srawley, J. E.: Fracture Tests of Surface Cracked Specimens of AMS 6434 Steel Sheet. Memo. Rep. 1097, Naval Res. Lab., Sept. 1960.

36. Srawley, J. E., and Beachem, C. D.: Fracture of High Strength Sheet Steel Specimens Containing Small Cracks. ASTM STP 302, Symposium on Evaluation of Metallic Materials in Design for Low-Temperature Service, 1962, pp. 69-83.

37. Yen, C. S., and Pendleberry, S. L.: Technique for Making Small Cracks in Sheet Metals. Materials Res. & Standards, vol. 2, no. 4, Nov. 1962, pp. 913-916.

38. Srawley, J. E.: Small Fatigue Cracks as Fracture Origins in Tests of High-Strength Steel Sheet. Proc. ASTM, vol. 62, 1962, pp. 734-741.

39. Green, A. E., and Sneddon, I. N.: The Distribution of Stress in the Neighborhood of a Flat Elliptical Crack in an Elastic Solid. Proc. Camb. Phil. Soc., vol. 46, Jan. 1950, pp. 159-163.

40. Sneddon, Ian N.: Crack Problems in Mathematical Theory of Elasticity. Rep. ERD-126/1, North Carolina State College, May 15, 1961.

41. Wundt, B. M.: A Unified Interpretation of Room-Temperature Strength of Notched Specimens as Influenced by Their Size. Paper 59-MET-9, ASME, 1959.

42. Steigerwald, E. A., and Hanna, G. L.: Initiation of Slow Crack Propagation in High-Strength Materials. Proc. ASTM, vol. 62, 1962, pp. 885-913.

43. Anctil, A. A., Kula, E. B., and DiCesare, E.: Electric-Potential Technique for Determining Slow Crack Growth. Proc. ASTM, vol. 63, 1963, pp. 799-808.

44. Praglin, J.: A Milli-Microvoltmeter. Keithley Eng. Notes, vol. 8, no. 4, Keithley Instr., Cleveland, Ohio, July 1960.

45. Van der Sluys, W. A.: Effects of Repeated Loading and Moisture on the Fracture Toughness of SAE 4340 Steel. T & AM Rep. 245, Univ. Ill., May 1963.

46. Boyle, R. W.: A Method for Determining Crack Growth in Notched Sheet Specimens. Materials Res. & Standards, vol. 2, no. 8, Aug. 1962, pp. 646-651.

47. Jones, M. H., and Brown, W. F., Jr.: Acoustic Detection of Crack Initiation in Sharply Notched Specimens. Materials Res. & Standards, vol. 4, no. 3, Mar. 1964, pp. 120-129.

48. Bulloch, D. F., and Ferguson, R.: Thick Section Fracture Toughness, Exhibit B. Quarterly Prog. Rep. 1, Boeing-North Am., Int. Airport, Los Angeles 9, Calif., Oct. 1963.

49. Romine, H. E.: Plane Strain Fracture Toughness Measurements of Solid Booster Case Materials, RTD-TDR-63-4048, Third Maraging Steel Proj. Rev., AF Materials Lab., Nov. 1963, pp. 185-211.

50. Morrison, J. D., Jenkins, P. C., and Kattus, J. R.: An Investigation of the Crack-Propagation Resistance of High-Strength Alloys and Heat-Resistant Alloys. Summary Tech. Rep. Dec. 23, 1960-Oct. 23, 1962, Southern Res. Inst., Nov. 21, 1962.

51. Kaufman, Albert: Performance of Electric-Resistance Strain Gages at Cryogenic Temperatures. NASA TN D-1663, 1963.

52. Kaufman, A.: Investigation of Strain Gages for Use at Cryogenic Temperatures. Experimental Mech., vol. 3, no. 8, Aug. 1963, pp. 177-183.

53. Romine, H. E.: Determination of the Driving Force for Crack Initiation from Acoustic Records of $\mathcal{G}_c$ Tests on High Strength Materials for Rocket Motor Cases. NWL Rep. 1770, Naval Weapons Lab., Oct. 4, 1961.

54. Kemp, R. H.: Characteristics and Application of Foil Strain Gages at -423° F. Paper presented at Western Regional Strain Gage Conf., Denver (Colo.), Sept. 30-Oct. 1, 1963.

55. Jones, M. H., and Brown, W. F., Jr.: An Axial Loading Creep Machine. ASTM Bull. 211, Jan. 1956, pp. 53-60.

"The aeronautical and space activities of the United States shall be conducted so as to contribute . . . to the expansion of human knowledge of phenomena in the atmosphere and space. The Administration shall provide for the widest practicable and appropriate dissemination of information concerning its activities and the results thereof."

—NATIONAL AERONAUTICS AND SPACE ACT OF 1958

NASA SCIENTIFIC AND TECHNICAL PUBLICATIONS

TECHNICAL REPORTS: Scientific and technical information considered important, complete, and a lasting contribution to existing knowledge.

TECHNICAL NOTES: Information less broad in scope but nevertheless of importance as a contribution to existing knowledge.

TECHNICAL MEMORANDUMS: Information receiving limited distribution because of preliminary data, security classification, or other reasons.

CONTRACTOR REPORTS: Technical information generated in connection with a NASA contract or grant and released under NASA auspices.

TECHNICAL TRANSLATIONS: Information published in a foreign language considered to merit NASA distribution in English.

TECHNICAL REPRINTS: Information derived from NASA activities and initially published in the form of journal articles.

SPECIAL PUBLICATIONS: Information derived from or of value to NASA activities but not necessarily reporting the results of individual NASA-programmed scientific efforts. Publications include conference proceedings, monographs, data compilations, handbooks, sourcebooks, and special bibliographies.

Details on the availability of these publications may be obtained from:

SCIENTIFIC AND TECHNICAL INFORMATION DIVISION

NATIONAL AERONAUTICS AND SPACE ADMINISTRATION

Washington, D.C. 20546